Title: Planarian dorsoventral Netrins control a muscle midline signaling center and regulate blastema formation

Authors and Affiliations:

Erik G. Schad[1,3]

Christian P. Petersen*[1,2]

1-Department of Molecular Biosciences, Northwestern University, Evanston, IL 60208

2-Robert Lurie Comprehensive Cancer Center, Northwestern University, Evanston IL 60208

3-present address: Genective, Weldon, IL 61882

*-corresponding author, christian-p-petersen@northwestern.edu

Abstract

Integration of positional information across body axes is likely critical for whole-body regeneration to define the territories of missing tissue in three dimensions with fidelity. The body-wall musculature in planarians expresses patterning factors regulating the anteroposterior, dorsoventral, and mediolateral axes, but how this information coordinates is not fully understood. We identify a previously described factor specifically expressed in dorsal midline muscle as a BMP/Activin decoy receptor *bambi-2*. Analysis of scRNAseq indicates *bambi-2*+ cells coexpress midline-specifying transcription factor *pitx* and longitudinal muscle-specifying factor *myoD*, and production of *bambi-2*+ cells requires these factors. In laterally amputated animals regenerating an entirely new midline, *bambi-2*+ cells are initially formed at the wound site, then dynamically spread, and ultimately reset to restore bilateral symmetry. We further identify a system of dorsoventral Netrin and Netrin receptor signals expressed from body-wall muscle that control midline identity and blastema morphology. Ventral and laterally expressed *netrins -1, -4,* and *-5* signal via dorsally-enriched netrin repulsion receptors *unc5-C, unc5-E,* and *dcc-2*, which together limit mediolateral spread of *bambi-2*+ dorsal midline muscle and influence the architecture of the muscle system. Our results suggest a model in which ventral determinants dictate mediolateral information important for blastema morphology.

Introduction

Whole body regeneration involves tissue restoration from a variety of possible truncations to axis content after amputation. Species of planarians, acoels, and cnidarians exemplify these abilities, as they are able to regenerate essentially entirely new animals after even severe injuries such as decapitation (Reddien, 2018; Vogg et al., 2019; Srivastava, 2022). The nature of robust positional information is therefore important to understand how extreme regenerative ability is possible. The information systems controlling regenerative ability across each body axis have often been considered separately, but surgical injuries also frequently damage more than one orthogonal body axis. How overall patterning across axes is accomplished

52 is incompletely understood and may be important for understanding how regenerative organisms correctly
53 match blastema specification to the identity and content of pre-existing tissue

54 Flatworm planarians can regenerate from nearly any type of surgical injury to restore axis content
55 along their anteroposterior (AP), dorsoventral (DV), and mediolateral (ML) axes. A system of posterior
56 Wnts and anterior Wnt inhibitors are expressed in gradients along the AP axis, and inhibition of canonical
57 Wnt signaling results in ectopic head regeneration while over-activation due to inhibition of anti-Wnt
58 factors results in ectopic tail regeneration (Gurley et al., 2008; Iglesias et al., 2008; Petersen and Reddien,
59 2008; Petersen and Reddien, 2009; Gurley et al., 2010; Petersen and Reddien, 2011; Owen et al., 2015;
60 Reuter et al., 2015; Stuckemann et al., 2017). In addition, two Wnt/FGFRL systems control head and trunk
61 regionalization in conjunction with Disheveled and Src signals (Cebria et al., 2002; Almuedo-Castillo et
62 al., 2011; Lander and Petersen, 2016; Scimone et al., 2016; Bonar et al., 2022). By contrast, the dorso-
63 ventral (DV) axis is controlled through dorsal *bmp4* signals and ventral *admp*, which signal in a negative
64 feedback loop (Molina et al., 2007; Orii and Watanabe, 2007; Reddien et al., 2007; Gavino and Reddien,
65 2011). Finally, medio-lateral axis patterning is regulated by medially expressed *slit* which opposes laterally
66 expressed *wnt5* (Cebria et al., 2007; Gurley et al., 2010).

67 The major signals specifying AP, DV, and ML pattern in planarians are expressed from
68 subepidermally located muscle body-wall cells that surround the inner parenchymal region containing the
69 neoblast planarian stem cells (Witchley et al., 2013). Neoblasts are pluripotent and generate all planarian
70 adult differentiated cells, thus underlying the animal's ability to replace diverse missing tissues and undergo
71 perpetual tissue homeostasis in the absence of injry (Wagner et al., 2011; Reddien, 2018; Zeng et al., 2018).
72 Planarian muscle cells are mononucleated and project contractile fibers across several orientations
73 (longitudinal, diagonal, circular, and dorsoventral orientations) to form a meshwork plexus (Witchley et al.,
74 2013; Cebria, 2016). The majority of patterning factors controlling regionalization are expressed from
75 multiple muscle subtypes (Scimone et al., 2017). However, analysis of cell fate transcription factors
76 required for producing individual muscle subtypes found that some patterning genes have expression
77 restricted to muscle oriented in particular directions. For example, injury triggers expression of the Wnt

78 inhibitor *notum* and the Activin pathway modulator *follistatin*, important for wound polarization and
79 outgrowth (Petersen and Reddien, 2011; Gavino et al., 2013; Roberts-Galbraith and Newmark, 2013;
80 Tewari et al., 2018), and inhibition of the longitudinal muscle fate transcription factor *myoD* prevents their
81 expression and leads to failed regeneration (Scimone et al., 2017). Likewise, circular muscle requires *nkx1.1*
82 for its production, selectively expresses *activin-2* involved in polarity determination (Cloutier et al., 2021),
83 and inhibition of *nkx1.1* leads to splitting the anterior pole and formation of split-axis animals (Scimone et
84 al., 2017). In addition, medial dorsoventral muscle controlled by *foxF1* and *gata4/5/6-2* factors is a source
85 of *slit* (Scimone et al., 2018). However, little is known about how the muscle system becomes organized
86 and how axis patterning systems communicate with each other to result in a restoration of form following
87 injury.

88 Prior studies have suggested the existence of communication across the body axes. The master
89 regulator of posterior identity *wnt1* is required for posterior regeneration and is expressed selectively in the
90 posterior along the dorsal midline (Petersen and Reddien, 2009; Gurley et al., 2010). *wnt1* is co-expressed
91 in a posterior subpopulation of dorsal midline (DM) muscle cells which express the previously unannotated
92 gene *dd23400* and extend across the majority of the AP axis (Fincher et al., 2018; Schad and Petersen,
93 2020). Overactivation of *wnt1* in *dd23400+* DM muscle cells through inhibition of *mob4* or *striatin*
94 components of the STRIPAK complex results in the expansion of posterior tissue in homeostasis and
95 regeneration, suggesting that regulation of DM muscle cells is important for body patterning (Schad and
96 Petersen, 2020). Additionally, the correct placement of the *notum+* anterior pole at the mediolateral and
97 dorsoventral midpoint is dependent on mediolateral components *wnt5* and *slit*, as well as the dorsoventral
98 regulator *bmp4* (Oderberg et al., 2017). These observations suggest that patterning information may
99 communicate across orthogonal axes and also the importance of the dorsal midline in regeneration.
100 However, the roles for dorsal midline muscle cells in regeneration are not fully understood.

101 In order to understand how midline cells contribute to regeneration, we analyzed single-cell
102 RNAseq data to identify factors expressed in midline muscle. This approach identified a set of transcription
103 factors required for DM muscle identity. We found that factors required for DM formation were also

104 required for lateral regeneration, suggesting the importance of these cells in facilitating outgrowth during
105 formation of a new mediolateral axis through regeneration. Furthermore, by tracking expression of midline
106 markers, we find that the re-establishment of dorsal midline during lateral regeneration proceeds from the
107 wound edge rather than the mediolateral center of the fragment. Using candidate approaches, analysis of
108 scRNAseq data, and functional analysis, we furthermore implicate Netrin related signals as regulators
109 restricting the domain of DM cells. Netrins are a class of secreted proteins known for their role in axonal
110 guidance (Hedgecock et al., 1990; Ishii et al., 1992; Kennedy et al., 1994; Serafini et al., 1994), and play a
111 role in axon growth and regeneration in planarians (Cebria and Newmark, 2005). Other known roles for
112 Netrins include cell survival (Mehlen et al., 1998; Llambi et al., 2001), organ morphogenesis (Dalvin et al.,
113 2003; De Breuck et al., 2003; Srinivasan et al., 2003; Yebra et al., 2003; Liu et al., 2004), and myotube
114 formation (Kang et al., 2004). In order to transduce their signals, Netrins bind a variety of targets including
115 UNC-5 (Hedgecock et al., 1990) and DCC (Chan et al., 1996; Keino-Masu et al., 1996; Kolodziej et al.,
116 1996; Fazeli et al., 1997). There are five genes encoding Netrins in planarians, all of which have prominent
117 expression in muscle cells and are regionally expressed across the ML and DV axes (Cebria and Newmark,
118 2005; Scimone et al., 2017; Fincher et al., 2018). In planarians, Netrin receptors (five UNC-5s, two DCCs)
119 are expressed widely, including in muscle cells (Fincher et al., 2018). Because Netrins and their receptors
120 are expressed in muscle cells regionally across the ML or DV axes like other genes controlling patterning
121 in planarians, we hypothesized that Netrins organize key features across these body axes, in particular, DM
122 muscle cells.
123
124 **Results**
125 *dd23400/bambi-2+* is expressed in dorsal midline muscle
126 To identify factors important for DM muscle, we sought genes expressed in this cell population. Prior
127 single-cell RNA seq analysis identified a gene *dd23400* expressed exclusively on the dorsal midline from
128 muscle cells. This gene was originally identified without discernable sequence similarity to other proteins
129 (Fincher et al., 2018). However, we noticed that PSI-blast of *dd23400* recovered several homologs of a

130 family of Bmp/Activin membrane-bound inhibitors (BAMBI) (Figure S1) whose members possess
131 extracellular ActR domains, lack intracellular activation domains, and may therefore function as decoy
132 receptors (Onichtchouk et al., 1999). SMART domain analysis weakly identified an ActR domain in
133 *dd23400* and also a transmembrane domain. Using maximum-likelihood phylogenies, *dd23400* placed with
134 strong support within a clade of bilaterian BAMBI homologs separate from BMPR1 receptors, and so we
135 named the gene *bambi-2*.

136 To examine the requirements for DM muscle cell production, we re-examined a prior whole-animal
137 single-cell RNAseq atlas generated by DropSeq to search for factors expressed in *bambi-2*+ muscle cells
138 (Fincher et al., 2018). Because *bambi-2* has relatively weak expression, we searched for cells co-expressing
139 *bambi-2* and the midline factor *slit,* and compared these to bulk muscle cells using the scde package for
140 differential gene expression profiling from single-cell RNAseq data (Kharchenko et al., 2014). The
141 resulting analysis identified several genes putatively enriched for expression in *bambi2*+ midline muscle
142 cells, including *pitx, bmp, msx, myoD, fgfr4, delta-like, TM211, nephrin, unc5-C,* and *fgfr4* (Figure 1A,
143 Table S1). A prior analysis using Smart-Seq to find transcriptome information for *wnt1*+ cells identified
144 enriched expression (log fold-change > 2) in these cells for *pitx, wif, nephrin, msx, fgfr4, bmp, myoD, unc5-*
145 *C, TM211, delta-like,* and *bambi-2* (Li et al., 2019). As a further test of midline enrichment, we performed
146 colorimetric whole-mount in situ hybridizations on several candidates to examine whether which had
147 midline expression. We found midline-related expression for 11 out of 15 factors tested, with the remaining
148 4 lacking detection in the assay (Figure 1A, Figure S1). The transcription factor *pitx* was identified
149 previously as important for expression of *wnt1* (Currie and Pearson, 2013; März et al., 2013), a master
150 regulator of posterior formation expressed from the posterior dorsal midline (Adell et al., 2009; Petersen
151 and Reddien, 2009; Gurley et al., 2010) and also for new expression of the midline determinant *slit* in
152 regeneration blastemas (Currie and Pearson, 2013; März et al., 2013). Posterior *wnt1* was subsequently
153 shown to be co-expressed in a posterior subset of *23400/bambi-2*+ dorsal midline muscle cells (Schad and
154 Petersen, 2020). We used FISH to verify that *pitx* has expression along the dorsal midline (Figure 1B). We
155 further reasoned that other factors required for *wnt1* expression might also have expression on the dorsal

156 midline. The transcription factor *islet* is required for expression of *wnt1* (Hayashi et al., 2011) and although
157 our analysis of a DropSeq atlas did not identify enrichment for this gene in midline muscle, a prior analysis
158 using SmartSeq found enrichment for *islet* expression in *wnt1*+ posterior midline cells (Li et al., 2019).
159 Using FISH, we found *islet* is expressed more broadly than *pitx,* but including dorsal midline cells in the
160 anterior and posterior of the animal (Figure 1B).

161 We observed that in addition to expression on the dorsal midline in the posterior, *islet* and *pitx* are
162 also expressed on the DM in the anterior (Figure 1B), so we reasoned that they could be required for all
163 *bambi-2*+ cells. We performed RNAi of *islet* and *pitx,* and found a nearly complete loss of *bambi-2*
164 expression (Figure 1C). *bambi-2*+ DM muscle cells may additionally be specified by transcription factors
165 required for other muscle cell subsets. The *myoD* transcription factor is required for longitudinal muscle
166 throughout the body (Scimone et al., 2017), was recovered by scRNAseq analysis as enriched in *bambi-2*+
167 midline cells, and its expression domain includes a midline-enriched region expression pattern (Figure 1A).
168 Therefore, we tested whether *myoD* inhibition would impact *bambi-2* dorsal muscle expression. RNAi of
169 *myoD*, but not the *nkx1.1* transcription factor required for circular muscle, caused a loss of *bambi-2*
170 expression, suggesting that *bambi-2*+ DM muscle cells are likely a subset of longitudinal muscle (Figure
171 1B). Because *pitx* and *islet* are known to be required for expression of *slit* (Currie and Pearson, 2013; März
172 et al., 2013), these results argue these factors likely control midline muscle cell identity in general. We
173 tested other markers of midline to confirm these findings. *dachsous* has midline expression (Vu et al.,
174 2019) and was enriched for expression in midline muscle by the scde analysis (Table S1, log2 upper-bound
175 enrichment of 3.10). *pitx* or *islet* RNAi resulted in a loss of *dachsous* expression (Figure 1D). Furthermore,
176 a homolog of *Wnt inhibitory factor (wif)* (Hsieh et al., 1999), itself a homolog of Drosophila *shifted* (Glise
177 et al., 2005), was recovered as strongly enriched in *bambi-2*+ muscle cells from the single-cell RNAseq
178 analysis (Figure 1A, log2 upper-bound enrichment of 10.92). FISH analysis revealed *wif* to be expressed
179 weakly along the dorsal midline, and inhibition of *pitx* or *islet* similarly reduced *wif* expression. Therefore,
180 *pitx* and *islet* are important for expression of several markers of dorsal midline muscle. We also used the
181 additional markers of midline muscle to examine the consequences of *bambi-2* inhibition on these cells.

182 *bambi-2(RNAi)* animals appeared phenotypically normal and did not fail to express midline *dachsous* or
183 *wif* (Figure 1C-D). Additionally, co-inhibition of another previously reported BAMBI homolog, *bambi* ,
184 also resulted in animals with normal appearance. Together, *bambi-2* is a marker of dorsal midline but likely
185 not critical for its formation.

186 The high specificity of expression of *bambi-2* for the dorsal midline enabled the opportunity to
187 examine the process of midline re-establishment during lateral regeneration. The expression of *bmp4* has
188 been used to examine midline formation during lateral regeneration previously. In *Schmidtea mediterranea*,
189 *bmp4* is expressed both on the dorsal midline as well as laterally on the dorsal side in a graded manner
190 (Reddien et al., 2007), and in *Dugesia japonica, bmp* expression is prominent on the midline and also
191 detectable in a graded fasion from the dorsal midline (Orii, 1998). In *Dugesia japonica* animals undergoing
192 lateral regeneration, *bmp4* expression punctate and broad at 1 day post amputation, which could either
193 reflect pre-existing or new expression of *bmp4* (Orii, 1998). By 3 days of regeneration, expression primarily
194 appeared as a line running anteroposteriorly and located asymmetrically on the fragment and closer to side
195 forming a regeneration blastema. As regeneration proceeded, the most abundant *bmp4* signal still appeared
196 to be asymmetric in the animal but located closer to the left-right midpoint of the fragment. Similar
197 asymmetry in *bmp4* expression early in regeneration has been reported in *Schmidtea mediterranea* with
198 some differences. In lateral regeneration in that organism, new expression of *bmp4* was detected at 12 hours
199 in a punctate pattern close to the wound site (Reddien et al., 2007). By 48 hours, expression was stronger
200 on the blastema side of the fragment but without yet a discernable midline component, and midline
201 expression could be detected by 14 days. Other tests of *bmp4* expression in lateral regeneration have
202 detected greater expression early in regeneration (2-4 days) on the blastema side of fragments (Gavino and
203 Reddien, 2011). Together, these prior observations suggest midline formation is unlikely to proceed through
204 a process that places new midline at the geometric midpoint. However, because *bmp* expression is graded
205 and includes non-medial dorsal cells, the exact nature of midline regeneration is still not fully understood.

206 We tested the expression of *bambi-2* during a timecourse of lateral regeneration in asymmetrically
207 laterally amputated fragments that unambiguously initially lacked midline expression. *bambi-2* expression

208 appeared by 24 hours at the wound edge at a location furthest from the existing lateral-most domain. *Bambi-*
209 *2* expression retained dorsal specificity throughout the timecourse, so this position would effectively mark
210 the dorsal-most position in the fragment remaining following the amputation (Figure 2). Over time, this
211 expression domain expanded while retaining dorsal specificity (100% of animals only had expression on
212 one DV side of the animal, N at least 8 animals per timepoint), reached a point of largest mediolateral
213 spread by 72 hours, followed by restriction to a location between the pre-existing tissue and growing
214 blastema. Consistent with prior studies, midline expression had not become fully restored to the middle of
215 the fragment by 7 days. These results support that dorsal midline regeneration proceeds initially in close
216 association with the wound site, followed by subsequent re-establishment.
217
218
219 <u>*Netrins from ventral/medial muscle domains coordinate to instruct blastema outgrowth shape*</u>
220 We hypothesized from these results that dorsoventral signals could be important for establishing
221 the *bambi-2*+ expression domain. We noticed that one of the genes enriched in midline muscle expression
222 from the scRNAseq analysis (*unc5*-C) belonged to the Netrin signaling pathway, suggesting a possible role
223 for this pathway in DM muscle function. Netrins are secreted proteins that provide guidance cues for
224 migratory cells (Hedgecock et al., 1990; Ishii et al., 1992) and can signal to receiving cells across long
225 ranges (Colavita and Culotti, 1998; Hong et al., 1999; Keleman and Dickson, 2001; Finci et al., 2014; Boyer
226 and Gupton, 2018). The planarian genome contains five genes encoding Netrin proteins, each expressed in
227 muscle cells (Figure 3A-C, Figure S2) (Fincher et al., 2018), while *netrin-1* and *netrin-2* are also expressed
228 in neurons (Cebria and Newmark, 2005; Scimone et al., 2017). Planarian Netrins are expressed in a series
229 of ML and DV domains (Figure 3A). *netrin-1* and *netrin-3* are coexpressed in *collagen*+ muscle cells on
230 the lateral edge of the animal, while *netrin-2* and *netrin-5* are expressed in medial muscle cells on the ventral
231 side (Figure 3A). *netrin-4* is expressed across the ventral side of the animal (Figure 3A). Sections of animals
232 co-stained with each Netrin and the muscle marker *collagen* showed that Netrins are expressed in several
233 ventral/medial domains within muscle. Because Netrins function in cell guidance and have graded

234 expression in muscle cells on the ML axis, we hypothesized that they play a role in organizing the DM
235 muscle domain. The planarian genome encodes several Netrin receptors: five putative UNC-5 receptors,
236 and two DCC receptors (Scimone et al., 2020). Each of these receptors is expressed broadly, but also has
237 graded expression in muscle cells (Fincher et al., 2018) (Figure 3B-C, Figure S2). *unc5-A,-B,-D* and *dcc-*
238 *1/net-R* are expressed on the lateral edge of the animal, while *unc5-C,-E* and *dcc-2* have prominent
239 expression in dorsal medial *collagen*+ muscle cells (Figure 3B-C). In summary, Netrins are expressed in
240 either lateral (*netrin-1,-3),* ventral-medial (*netrin 2,-5*), or broad ventral (*netrin-4*) domains, while putative
241 receptors are expressed in lateral (*unc5-A,-B,-D* and *dcc-1/net-R*) or dorso-medial (*unc5-C,-E* and *dcc-2*)
242 domains (Figure 3D).

243 To investigate the role of Netrins during regeneration we inhibited each Netrin using RNAi. We
244 first inhibited each Netrin individually, resulting in no overt phenotypes of dysfunction in either anterior or
245 posterior regeneration (Figure 4A). We reasoned that Netrins could function redundantly, and so we
246 inhibited all five planarian Netrins through combined RNAi, and verified by qPCR for effective knockdown
247 (Figure S3). Inhibition of all Netrins simultaneously resulted in regeneration with midline defects of a
248 pointy blastema in the anterior (32/36 regenerating trunk fragments), and of indented blastemas in the
249 posterior (7/36) (Figure 4B). In addition, at a low frequency, inhibition of the five Netrins resulted in failed
250 anterior regeneration in amputated tail fragments (6/36) or failed posterior regeneration from amputated
251 head fragments (5/36 animals). We reasoned that these phenotypes were either due to inhibition of all
252 Netrins together or instead due to inhibition of subsets of Netrins. To test this hypothesis, we inhibited each
253 possible combination of two, three, or four Netrins, and scored animals for the penetrance and expressivity
254 of pointy blastema in anterior blastemas or indentations in posterior blastemas (Figure S4A-B). We found
255 that inhibition of all combinations of Netrins resulted in anterior pointy blastemas to varying degrees.
256 Inhibition conditions including RNAi of *netrin-4,-5* yielded the strongest effects on pointy blastemas,
257 followed by those including *netrin-1* and *netrin-2*. The laterally expressed *netrin-3* factor likely did not
258 contribute, because *netrin-1;-2;-3;-4;-5* RNAi yielded the same outcome as *netrin-1;-2;-4;-5* RNAi (Figure
259 S4A). Therefore, *netrin-1, -2 ,-4,* and *-5* contribute to normal anterior regeneration morphology.

260 A similar analysis of the indented blastema phenotype from posterior-facing wounds found a
261 somewhat distinct outcome. Whereas inhibition of all five Netrins simultaneously resulted in an indented
262 blastema, inhibition of most combinations of Netrins resulted in normal posterior regeneration. Inhibition
263 of *netrin-1, -4,* and *-5* increased the penetrance and expressivity of indentation over that from inhibition of
264 all netrins, indicating a particular importance for these three genes in enabling midline regeneration in the
265 posterior (Figure S4B). Consistent with this model, RNAi combinations excluding inhibition of any of these
266 three Netrins resulted in normal posterior regeneration, and co-inhibitions with *netrin-2* or *netrin-3* did not
267 strongly affect the outcome. Therefore, *netrin-1*, *netrin-4*, and *netrin-5* act together to ensure midline
268 regeneration in blastemas generating posterior tissue.

269 We also examined whether the low frequency of failed regeneration after inhibition of all Netrins
270 simultaneously could be explained by lack of injury-induced gene expression from muscle cells. However,
271 *netrin-1;-2;-3;-4;-5(RNAi)* animals had normal injury-induced expression of *notum* and *follistatin* (Figure
272 S5). We suggest that the failed regeneration phenotype could either reflect a distinct role for Netrins or a
273 more extreme version of the defects causing impaired blastema morphology. Nonetheless, these results
274 suggest that Netrin inhibition does not result in failed responsiveness of longitudinal muscle cells to injury
275 (Scimone et al., 2017). These results also suggest that the indented morphology phenotype is not likely due
276 to a problem with early expression of injury-induced *notum* or *wnt1*.

277 To further investigate the role of Netrin signaling in regeneration, we conducted RNAi experiments
278 to test for functions of the Netrin receptors. Inhibition of the receptors expressed in lateral domains (*unc5-*
279 *A,-B,-D* and *dcc-1/net-R*) appeared to result in normal regeneration, including when inhibited in
280 combination (Figure 4C). However, inhibition of either *unc5-C, unc5-E*, or *dcc-2* caused regeneration with
281 indentations to posterior blastemas in all cases, and indentations to anterior regeneration after *dcc-2* RNAi.
282 Dual inhibition of *unc5-E* and *unc5-C* or triple inhibition of *unc5-E;unc5-C;dcc-2* resulted in more strongly
283 expressive anterior and posterior blastema indentations. The indented posterior blastemas were reminiscent
284 of the posterior blastema morphology phenotypes after RNAi of *netrins-1, -4,* and *-5*, suggesting these
285 Netrins may signal through *unc5-E/unc5-C/dcc-2* receptors. Furthermore, while *netrin-1, netrin-4* and

286 *netrin-5* have expression in ventral and lateral muscle domains, *unc5-E* and *unc5-C* have enrichment in a
287 dorsal domain (Figure 3). These observations implicate a system of Netrin ligands and receptors signaling
288 across muscle domains in to control midline blastema morphology.
289
290 Netrins act as repulsive signals to restrict the midline domain
291 Based on the overt mediolateral defects in blastema formation after Netrin RNAi, we tested the
292 expression of ML and DV patterning factors in these animals. *netrin-1;-2;-3;-4;-5(RNAi)* animals displayed
293 an increase in *bambi-2* domain width, especially in the anterior (Figure 5A). Similarly, midline expression
294 of *slit* was also expanded in *netrin-1;-2;-3;-4;-5(RNAi)* animals, while laterally expressed *wnt5* was
295 unchanged (Figure 5A-C). Furthermore, *netrin-1;-2;-3;-4;-5(RNAi)* animals retained expression of dorsal
296 *bmp4* and ventral expression of *admp*, suggesting these animals did not undergo ventralization or
297 dorsalization (Figure 5A). Finally, *netrin-1;-2;-3;-4;-5(RNAi)* animals succeeded in expressing *wnt1+* at
298 the posterior pole and *notum* at the anterior pole, consistent with animals regenerating with normal head
299 and tail identity in spite of the blastema morphology defects (Figure 5A). We noted that although *notum*
300 expression was correctly located at the anterior pole, its expression was expanded over the Netrin(RNAi)
301 pointy blastema compared to controls. Prior studies suggest that a preexisting midline can determine the
302 location of a newly regenerated anterior pole (Oderberg et al., 2017), so perhaps the expanded midline
303 domain in *netrin-1;-2;-3;-4;-5(RNAi)* animals may cause formation of an expanded anterior pole. Together,
304 these findings implicate Netrins specifically in restricting dorsal midline identity. Based on these findings,
305 we specifically tested for any midline defects after inhibition of the Netrin receptors involved in midline
306 formation. Simultaneous RNAi of *unc5-C, unc5-E,* and *dcc-2* resulted in a similar expansion of the *bambi-*
307 *2+* cell domain (Figure 3B-C). Therefore, the phenotypes of dorsal midline expansion correlate with
308 indented blastemas. Reception of Netrins through receptor heterodimers of Unc5 and DCC family members
309 are thought to signal repulsion during axon guidance and cell migration (Lai Wing Sun et al., 2011).
310 Furthermore, the *bambi-2+* dorsal midline cells are located at the point furthest away from the sources of
311 ventral and medial *netrin-1, netrin -4* and *netrin-5* but within the dorsal domains of *unc5-E* and *unc5-C*

312 expression. Therefore, we suggest that the *bambi-2*+ cells are restricted dorsally because of repulsive
313 signaling between ventral/lateral *netrin-1,-4,-5* to dorsally expressed Unc5 receptors *unc5-E* and *unc5-C*
314 signaling through *dcc-2.*

315 The expression of Netrins within muscle cells led us to hypothesize that Netrins might control some
316 aspect of organization of the muscle fiber network important for blastema formation in regeneration. To
317 test this hypothesis, we inhibited all Netrins or Netrin receptors *unc5-E, unc5-C,* and *dcc-2*, and then used
318 immunofluorescence to label animals with a monoclonal antibody (6G10) that labels muscle cell fibers
319 (Ross et al., 2015) (Figure 5D). In *netrin-1,-2,-3,-4,-5(RNAi)* animals, muscle cell fibers were present in the
320 pointed anterior blastemas and appeared normal, although they appeared to track with the overall pointed
321 morphology. In *netrin-1,-2,-3,-4,-5(RNAi)* animals, some circular muscle fibers near the indented posterior
322 regenerated tissue inappropriately projected anteroposteriorly after crossing the midline. *unc5-E;unc5-*
323 *C;dcc-2* RNAi led to a more severe defect of indentation, and we also noticed such animals have a zone of
324 muscle disorganization immediately anterior to the indentation along the midline, which could reflect a
325 muscle remodeling process linked to indented tissue. We conclude that a system of ventrally expressed
326 Netrins and dorsally expressed Netrin Receptors are likely not required for muscle fiber growth altogether,
327 but impact the architecture of the muscle system.

328

329 **Discussion**

330 Whole-body regeneration requires the re-establishment of patterning across all major body axes.
331 Here, we identify processes important for generating, restricting, and using *bambi-2*+ dorsal midline muscle
332 in planarian regeneration. Inhibition of factors *pitx* and *islet* caused loss of midline expression of *bambi-2,*
333 *dachsous,* and *wif* and also prevented blastema outgrowth during lateral regeneration, suggesting the
334 importance of these cells in restoring mediolateral tissue distribution. We furthermore used *bambi-2*
335 expression as a probe to uncover the overall process of midline regeneration from fragments lacking a
336 midline. *bambi-2* expression initiates at the lateral wound edge. Subsequently, *bambi-2* expression expands

337 then appears to restrict to a region between new and old tissue, and differential growth over several weeks
338 ultimately restores bilateral symmetry (Figure 6A).

339 In addition, we describe the essential role of Netrin signaling in ML patterning during regeneration
340 in planarians (Figure 6B). *netrin-1,-2,-3,-4,-5* inhibition lead to an expansion of the *bambi-2+* cell domain,
341 but did not alter overall DV or AP identities. Netrins are known for their role in axonal growth (Hedgecock
342 et al., 1990; Ishii et al., 1992; Hamelin et al., 1993; Colavita and Culotti, 1998), including in planarians
343 (Cebria and Newmark, 2005), but Netrins can also guide myotube formation and other migrating cells in
344 murine development (Dalvin et al., 2003; De Breuck et al., 2003; Srinivasan et al., 2003; Yebra et al., 2003;
345 Kang et al., 2004; Liu et al., 2004), so it is plausible that Netrins may function to guide muscle cell growth
346 in planarians. Three putative Netrin receptors (*unc5-C, -E, dcc-2*) are expressed in dorso-medial muscle
347 cells, and their inhibition leads to an expansion of the *bambi-2+* cell domain. These results are consistent
348 with a model in which ventral Netrins act as repellants by binding to these receptors (Figure 6B). When
349 *netrin-1,-2,-3,-4,-5* are inhibited together, anterior blastemas form with a pointed morphology, with
350 expanded *notum+* anterior pole cells. Prior work determined that the midline instructs where the anterior
351 pole is placed in the anterior blastema (Oderberg et al., 2017), suggesting that the expanded dorsal muscle
352 domain from Netrin RNAi conditions may cause the regeneration of an excessively wide anterior pole, thus
353 generating pointed blastemas. Alternatively, it is possible that the pointy blastema phenotype represents a
354 loss of other outputs for Netrin activity. For example, Netrins can function as attractants in axon guidance
355 or migration, and this function is thought to occur via DCC/DCC receptor dimers rather than DCC/Unc5
356 dimers (Lai Wing Sun et al., 2011). In our survey of Netrin receptor RNAi phenotypes, no condition
357 phenocopied the pointy blastema defect observed from Netrin RNAi. One possible explanation could be
358 that due to the shared use of DCC in both repulsion and attraction, it is not possible to use RNAi of these
359 factors to selectively disrupt the process of attraction. Alternatively, perhaps other receptors are the targets
360 of Netrin signaling disrupted during the acquisition of the pointy blastema phenotype. Along these lines,
361 we also did not find blastema failure phenotypes through inhibition of Netrin receptors. However, our
362 phenotypic analysis identified shared functions in controlling the regeneration of midline tissue in the

363 posterior as well as in muscle targeting, for a subset of Netrins and Netrin receptors. RNAi of *netrin-1;-4;-*
364 *5* or *unc5-C;unc5-E;dcc-2* impacted the organization of the planarian musculature system, causing the
365 newly made circular muscle in regenerating blastemas to mistarget over the midline and instead forming
366 separated domains that grow into indented blastemas.

367 Whole body regeneration in planarians depends on axis information systems encoded in muscle
368 cells. Our study finds muscle-expressed ligands signaling through muscle-expressed receptors to control
369 regionalization of muscle identity. These observations suggest that regionalization signaling could take
370 place directly between muscle cells. Alternatively, given that *dcc-2* and other netrin receptors are expressed
371 more broadly, an alternative possible mechanism for pattern formation could involve the use of positional
372 cues from muscle to influence regionalization through control of stem cell differentiation into distinct
373 muscle domains. Netrins have dorsoventral expression domains opposing BMP in multiple organisms,
374 including in planarians (Cebria et al., 2007; Reddien et al., 2007), hemichordates (Lowe et al., 2006), acoels
375 (Srivastava et al., 2014), Drosophila (Harris et al., 1996; Mitchell et al., 1996), and within the vertebrate
376 neural tube (Serafini et al., 1994; Lai Wing Sun et al., 2011). In addition, Netrins have expression in body
377 wall muscle in planarians (Witchley et al., 2013), acoels (Raz et al., 2017), *Drosophila*, and *C. elegans*
378 (Ishii et al., 1992). Our observations point to an ancient and conserved use of Netrins for linking
379 dorsoventral and midline identity through muscle. The involvement of multiple Netrins and receptors for
380 controlling dorsal midline muscle and blastema morphology suggests the possibility of a dorsoventral code
381 of these factors that guide patterning of the blastema in order to restore bilateral symmetry during whole-
382 body regeneration.

383

384 **Acknowledgements**

385 We thank members of the Petersen lab for critical comments. CP acknowledges funding from NIGMS
386 R01GM129339, R01GM130835, and pilot project funding from the NSF-Simons Center for Quantitative
387 Biology at Northwestern University, an NSF (1764421)-Simons/SFARI (597491-RWC) MathBioSys
388 Research Center.

389

390 **Author contributions:** CP conceived of the study and acquired funding, ES designed and conducted
391 experiments, CP and ES wrote the manuscript.

392

393 **Declaration of Interests:** There are no competing interests.

394

395

396

397 **Figure Legends**

398 **Figure 1. *pitx, islet,* and *myoD* are required for expression of *bambi-2*.**

399 **(A)** Analysis of prior scRNAseq data (Fincher et al 2018) comparing transcriptomes of dorsal muscle
400 midline cells co-expressing *bambi-2(dd23400)* and *slit* versus *collagen+* muscle lacking *bambi-2* and *slit*
401 expression. Table shows log2-fold change (upper bound, ub) from scde analysis. Right panels show WISH
402 of candidates with expression on the posterior midline. Images represent 3-4 animals per condition. **(B)**
403 Animals were fixed and FISH was performed to detect *islet* or *pitx* expression on the dorsal midline in the
404 anterior (left) or posterior (right). Arrows indicate expression on the dorsal midline. **(C)** Homeostatic RNAi
405 (8 feedings dsRNA) to inhibit transcription factors specific for midline cells (*islet, pitx*), L-muscle (*myoD*),
406 and C-muscle (*nkx1-1*) followed by FISH to detect *bambi-2*. **(D)** FISH to detect expression of *dachsous* and
407 *wif* midline markers after *pitx*, *islet* or *bambi-2* RNAi**.** Bars, 100 (B) or 200 microns (A,C).

408

409

410

411

412 **Figure 2. Lateral regeneration progressively restores *bambi-2* midline expression through injury-**
413 **induced expression and growth.**

414 FISH of *bambi-2* expression during a timeseries of the regeneration of asymmetric lateral fragments that
415 must regenerate the dorsal midline. Bottom, quantifications of the relative and absolute locations of the
416 *bambi-2*+ cells with respect to the wound edge (left), the relative size of the *bambi-2*+ domain and size of
417 pre-existing tissue domain lateral to the *bambi-2* domain (center), and absolute width of the regenerating
418 fragments. *bambi-2* expression first arises at the lateral wound edge by 24 hours, followed by a
419 progressive relative movement toward the left/right center of the fragment, rather than a mechanism that
420 directly places these cells centrally. n=12-15 animals. * $p<0.05$, ** $p<0.01$, *** $p<0.001$ by two-tailed
421 unpaired t-tests.
422
423 **Figure 3. Netrins and Netrin receptors are expressed in dorsoventral domains in muscle cells.**
424 **(A)** FISH images showing *netrins* are expressed in along either ventromedial (*netrin-2, netrin-4, netrin-5)*
425 or lateral (*netrin-1, netrin-3)* domains. Each image shows a ventral view. N=5-6 animals. **(B)** FISH images
426 showing Netrin receptors are expressed in along either dorsomedial (*unc5-C, unc5-E, dcc-2)* or lateral
427 (*unc5-A, unc5-B, unc5-D, dcc-1)* domains (4-7 animals probed per condition). (C) Images of cross-sections,
428 dorsal side top. FISH images showing *netrins* are expressed in along either ventromedial (*netrin-2, netrin-*
429 *4, netrin-5)* or lateral (*netrin-1, netrin-3)* domains (4-6 animals probed per condition) FISH images showing
430 Netrin receptors are expressed in along either dorsomedial (*unc5-C, unc5-E, dcc-2)* or lateral (*unc5-A, unc5-*
431 *B, unc5-D, dcc-1)* domains. Bars, 100 (A,B) or 50 microns (C). Arrows indicate expression of each tested
432 gene coincident with *collagen*+ muscle. (D) Cartoon of planarian cross-section displaying the approximate
433 expression domains for each Netrin and Netrin receptor.
434
435 **Figure 4. Netrins act cooperatively to control blastema morphology and regeneration.**
436 **(A)** Live images showing RNAi of individual *netrins* results in normal regeneration. (10 animals per
437 condition). **(B)** Simultaneous inhibition of all five Netrins causes regeneration of blastemas with an
438 indentation in the posterior and pointed morphology in the anterior, as well as weakly penetrant

439 regeneration failure in head and tail fragments (arrows). **(C)** RNAi of *unc5-C, unc5-E* and *dcc-2*
440 individually or in combination results in indented blastemas (arrows). Bars, 200 microns.
441
442 **Figure 5. Netrins control midline muscle cell organization and proper muscle morphology.**
443 **(A)** FISH showing expression of patterning factors following inhibition of each Netrin. Midline (*bambi-2,*
444 *slit*) and anterior pole cells (*notum)* are expanded, while lateral (*wnt5*), posterior (*wnt1*), and dorsoventral
445 markers (*bmp-4, admp-1*) appear normal. *admp-* and *notum*-stained animals are from regenerating tail
446 fragments, all other panels show regenerating trunk fragments. Insets show enlargements of *bambi-2* and
447 *slit* expression **(B)** FISH showing expanded *bambi-2* expression domain following *unc5-C,-E,dcc-2* RNAi.
448 Insets show enlargements of *bambi-2* expression. **(C)** Quantification of midline expansion normalized to
449 body width in each condition. Bars show standard error of 5-10 replicates, *** $p < 0.001$ by 2-tailed unpaired
450 t-test. **(D)** Immunostaining with 6G10 antibody to visualize muscle fiber morphology after *netrin-1;-2;-3;-*
451 *4;-5* RNAi and *unc5-C;unc5-E;dcc-2* RNAi in anterior (top) or posterior (bottom) blastemas. Muscle
452 morphology was disrupted at locations of the indented blastema. Animals were fixed after 8 dsRNA
453 feedings and 14 days of regeneration in all panels. Bars, 200 (A-B) or 100 microns (D).
454
455 **Figure 6. Model**
456 **(A)** In regeneration of lateral fragments, the *bambi-2*+ dorsal midline muscle is re-established near the
457 wound site and not the geometric center of the fragment. *pitx* and *islet* are necessary both for *bambi-2*
458 expression and blastema outgrowth that restores bilateral symmetry (B) Three ventral netrins likely act
459 through dorsal netrin receptors to restrict the location of the *bambi-2*+ cells.
460
461
462
463
464 **Supplemental Figures**

465 **Figure S1. dd23400/*bambi-2* encodes a BAMBI decoy receptor**

466 **(A)** Sequence alignment of dd23400 with BAMBI factors with conserved residues highlighted in red. Green bar
467 indicates location of ActR domain. dd23400 has a weakly detected ActR domain (aa4-84, evalue 0.14), possesses
468 a transmembrane domain (aa158-180, TMHMMv2.0) and like other BAMBI homologs lacks an intracellular
469 kinase activation domain. DELTA Blast of dd23400 followed by PSI-blast (3 rounds, 500 iterations) recovers
470 BAMBI orthologs from several species, including BAMBI from Osmia bicornis (evalue=1e-22), Megachile
471 rotundata (evalue=3e-22) and Apis mellifera (evalue=3e-20).**(B)** Bayesian inference phylogenetic tree generated
472 from alignment with MUSCLE and calculated with MrBayes v3.2.3 using a GTR substitution model with
473 gamma-distributed rate variation across sites and a proportion of invariable sites. Runs of 50000 generations
474 converged with an average standard deviation of split frequencies <0.01 and 25% of trees were discarded as
475 burn-in. Tree displayed using FigTree v1.4.4 with branch labels indicating posterior probabilities. BAMBI
476 sequences from Owenia fusiformis (Of, CAC9588793.1), Octopus bimaculoides (Ob, XP_014790456.1),
477 Argiope bruennichi (Ab, KAF8794778.1), Araneus ventricosus (Av, GBL98371.1), Stegodyphus mimosarum
478 (Sm, KFM81221.1), Xenopus laevis (Xl, CAB56858.1), Mus musculus (Mm, NP_036474.1), and
479 Branchiostoma floridae (Bf, XP_035688850.1).Tree is rooted using BMPR1 receptors from Brachiostoma
480 floridae (Bf), Danio rerio (Dr), and Mus musculus (Mm).

481

482 **Figure S2. Expression of netrins and netrin receptors from cell atlas.**

483 Plots of Netrin and Netrin receptor gene expression from a planarian cell atlas (Fincher et al., 2018 ;
484 digiworm.wi.mit.edu). Top cartoon shows cluster identities. Netrins and receptors have expression in
485 muscle cells and also in other cell types.

486

487 **Figure S3. qPCR validating knockdown.**

488 dsRNAs targeting netrins -1, -2, -3, -4, and -5 were mixed together and delivered to animals by feeding 6
489 times over 2 weeks ("pan-net") and compared to animals treated with control dsRNA. RNA was harvested

490 and qPCR conducted to measure knockdown of each Netrin factor as indicated, using *clathrin* transcript as
491 a normalizing control. Bars show standard error of 4 replicates, ***P<0.001 by 2-tailed unpaired t-test.
492
493 **Figure S4. Netrins -1, -2, -4, and -5 promote proper anterior blastema morphology while *net-2, -4,***
494 **and -5 promote posterior blastema morphology.**
495 (A) Graph showing regeneration score of anterior blastemas for all combinations of Netrin RNAi. n=7-10
496 animals. Animals were qualitatively scored based on the degree of pointedness from P0 (normal), P1
497 (subtle), P2 (pointy), to P3 (highly pointed). In order to compare different conditions with varying
498 penetrance and expressivity, a weighted average phenotype strength score was computed for each treatment
499 by summing the numbers of animals scored in each category multiplied by a scalar of increasing size for
500 higher expressivity (i.e., score = [(# animals in P1) + 2 x (# animals in P2) +3 x (# animals in P3)]/(total
501 number scored)). Average phenotype strength scores were normalized to the value from inhibition of all
502 five Netrins for comparison. Right- Representative images of degrees of blastema pointedness in different
503 combinations of Netrin inhibitions. (B) Graph showing percentage of indented posterior blastemas for all
504 combinations of Netrin RNAi. n=7-10 animals. Right- Representative images of degrees of indented-ness
505 in different combinations of Netrin inhibitions. (C) Live images showing *netrin-1;-2;-3;-4;-5* are not
506 required for blastema formation in regenerating fragments lacking midline.
507
508 **Figure S5. *netrins* are not required for wound-induced expression of *notum* and *follistatin.***
509 **(A)** Animals were fixed following 8 dsRNA feedings and fixed either 6 or 24 hours after injury. FISH
510 showing *notum* or *fst* expression is unchanged in All Netrin RNAi. n=>10 animals. In panel A bars are 200
511 microns.
512
513
514 **Materials and Methods**
515 **Experimental Model**

516 Asexual *Schmidtea mediterranea* animals (CIW4 strain) were maintained in 1x Montjuic salts
517 between 18–20°C. Animals were fed a puree of beef liver and starved for at least 7 days before experiments.
518
519 **In situ hybridizations**
520 Animals were fixed and bleached as described previously (Pearson et al., 2009; King and Newmark, 2013).
521 Riboprobes (digoxigenin- or fluorescein-labeled) were synthesized by in vitro transcription (Pearson et al.,
522 2009; King and Newmark, 2013). Antibodies were used in TNTx/10% horse serum
523 (Roche, Basel Switzerland) at a concentration of 1:2000 for anti-DIG-POD (Roche, Basel Switzerland),
524 and 1:2000 for anti-FL- (Roche), or 1:4000 for anti-dig-alkaline phosphatase used in colorimetric in situ
525 hybridizations (Roche, Basel Switzerland). For multiplex FISH, peroxidase conjugated enzyme activity
526 was quenched between tyramide reactions by sodium azide treatment (100 mM in 1xTNTx) for 45 min at
527 room temperature. Nuclear counterstaining was performed using Hoechst 33342 (Invitrogen, 1:1000 in
528 1xPBSTx for 45 minutes). Colorimetric in situ hybridizations were developed using NBT/BCIP as
529 described previously (Lander and Petersen, 2016). Primer sequences used for cloning to generate riboprobes
530 are listed in Table S2.
531
532 **Immunostaining**
533 Animals were fixed the same as in FISH (King and Newmark, 2013). Bleaching was performed in
534 80% methanol, 20% hydrogen peroxide on a lightbox overnight. Following rehydration washes, animals
535 were washed and rocked in PBSTx/10% horse serum (Roche, Basel Switzerland) 8 times for 6 hours.
536 Animals were incubated in the anti-muscle mouse monoclonal antibody 6G10-2C7 (Iowa Hybridoma Bank)
537 at 1:1000 overnight, then washed in PBSTx/10% horse serum 8 times for 6 hours. Animals were incubated
538 overnight in an anti-mouse Dig conjugated antibody in PBSTx/10% horse serum. After 8 PBSTx washes,
539 tyramide amplification was performed using commercial tyramide kit. Finally, animals were washed in
540 PBSTx 8 times, 20 minutes each.
541

542 **RNAi administration**

543 RNAi by feeding was performed in vitro transcribed dsRNA mixed with liver paste and 5% red
544 food dye (Rouhana et al., 2013). For single RNAi experiments, dsRNA at a concentration of 2-4 ug/ul was
545 mixed with liver in a 1:5 ratio. In RNAi experiments with multiple dsRNAs, each dsRNA was mixed with
546 liver for a total concentration of 1:10 for each dsRNA. In all RNAi experiments animals were fed RNAi
547 food every 2-4 days for the length of experiment indicated. For homeostatic experiments, animals were
548 starved for at least 5 days before fixing. In regeneration experiments, animals were amputated the same day
549 of the last feeding, or in Figure 1C, 1D, Figure S4 at 5 days after the final RNAi feeding. dsRNA targeting
550 the *Photinus pyralis* luciferase (not present in the planarian genome) was used as a negative control RNAi
551 condition. Primers sequences used for RNAi are listed in Table S2.

552

553 **Image Acquisition and Quantification**

554 Live images of animals were performed with a Leica M210F dissecting scope with a Leica DFC295 camera.
555 FISH images were performed a Leica DM5500B compound microscope with optical sectioning by Optigrid
556 structured illumination or a Leica Stellaris or Leica TCS SPE confocal compound microscopes. Fluorescent
557 images collected by compound microscopy are maximum projections of a z-stack and adjusted for
558 brightness and contrast using Metamorph, Adobe Photoshop, ImageJ, or Leica LAS.

559

560 **qPCR**

561 RNA was harvested from 4 biological replicates of 4 animals per condition using a Turrex tissue
562 homogenizer. cDNAs were synthesized using oligo-dT and Superscript III reverse transcriptase (Life
563 Technologies) for 1 hour at 50°C. EvaGreen qPCR mastermix (Midwest Scientific BEQPCR-S) was used
564 for amplification and detection. Per-sample log2-fold change expression were determined by the delta-
565 delta Ct method, normalizing to expression of housekeeping gene clathrin probe set control and to RNAi
566 negative controls targeting *Photinus pyralis* luciferase (not present in planarian genome). Statistical
567 significance was determined through unpaired two-tailed t-tests comparing ddCt values between control

568 RNAi and target RNAi conditions. Primers for qPCR: *netrin-1* (5'-taaagagcatcagggtctatgtga -3', 5'-
569 ataatatcgacgcttcaatttcca-3'); *netrin-2* (5'-gaattggtatgacaagacaactgc-3', 5'-gttttgcgtcgcatatactacaat-3');
570 *netrin-3* (5'-cgaaaccctatgtaaaaagaagga-3', 5'-cccttggagattttataggacaga-3') ; *netrin-4* (5'-
571 cctgttaaattgaaatcgctctct-3', 5'-aataaaataatttggggatgctga-3') ; *netrin-5* (5'-tgcacaaaatgctacatttgaagt-3', 5'-
572 atcctttctgaccgcatgtact-3'); *clathrin* (5'-agccgcatgtagttggttagtg-3', 5'-agtctacagaaaaccatcaattgtttcaaa-3').
573

574 **scRNAseq differential gene expression testing**

575 We mined a prior single-cell RNAseq atlas generated by DropSeq (Fincher et al., 2018) and recovered 15
576 *dd23400+slit+* cells (at least 1 read for *bambi-2/dd23400* and at least 2 reads for *slit*) and compared these
577 to 143 randomly selected muscle cells (at least 7 reads for muscle marker *collagen* dd840 and no reads for
578 *dd23400* or *slit*) and analyzed for differential gene expression using the Single Cell Differential Gene
579 Expression (scde) method (Kharchenko et al., 2014). Table S1 shows results of differential testing along
580 with identity of cells selected for analysis.
581

582 **Phylogenetic analysis**

583 Bayesian inference phylogenetic tree was generated from alignment with MUSCLE and calculated with
584 MrBayes v3.2.3 using a GTR substitution model with gamma-distributed rate variation across sites and a
585 proportion of invariable sites. Runs of 50000 generations converged with an average standard deviation of
586 split frequencies <0.01 and 25% of trees were discarded as burn-in.
587
588
589
590

591 **References**
592

593 ADELL, T., SALÒ, E., BOUTROS, M. & BARTSCHERER, K. 2009. Smed-Evi/Wntless is
594 required for β-catenin-dependent and-independent processes during planarian
595 regeneration. *Development,* 136**,** 905-910.
596 ALMUEDO-CASTILLO, M., SALÓ, E. & ADELL, T. 2011. Dishevelled is essential for neural
597 connectivity and planar cell polarity in planarians. *Proceedings of the National Academy*
598 *of Sciences,* 108**,** 2813-2818.
599 BONAR, N. A., GITTIN, D. I. & PETERSEN, C. P. 2022. Src acts with WNT/FGFRL signaling
600 to pattern the planarian anteroposterior axis. *Development,* 149.
601 BOYER, N. P. & GUPTON, S. L. 2018. Revisiting Netrin-1: One Who Guides (Axons). *Front*
602 *Cell Neurosci,* 12**,** 221.
603 CEBRIA, F. 2016. Planarian Body-Wall Muscle: Regeneration and Function beyond a Simple
604 Skeletal Support. *Front Cell Dev Biol,* 4**,** 8.
605 CEBRIA, F., GUO, T., JOPEK, J. & NEWMARK, P. A. 2007. Regeneration and maintenance of
606 the planarian midline is regulated by a slit orthologue. *Dev Biol,* 307**,** 394-406.
607 CEBRIA, F., KOBAYASHI, C., UMESONO, Y., NAKAZAWA, M., MINETA, K., IKEO, K.,
608 GOJOBORI, T., ITOH, M., TAIRA, M., SANCHEZ ALVARADO, A. & AGATA, K.
609 2002. FGFR-related gene nou-darake restricts brain tissues to the head region of
610 planarians. *Nature,* 419**,** 620-4.
611 CEBRIA, F. & NEWMARK, P. A. 2005. Planarian homologs of netrin and netrin receptor are
612 required for proper regeneration of the central nervous system and the maintenance of
613 nervous system architecture. *Development,* 132**,** 3691-703.
614 CHAN, S. S., ZHENG, H., SU, M. W., WILK, R., KILLEEN, M. T., HEDGECOCK, E. M. &
615 CULOTTI, J. G. 1996. UNC-40, a C. elegans homolog of DCC (Deleted in Colorectal
616 Cancer), is required in motile cells responding to UNC-6 netrin cues. *Cell,* 87**,** 187-95.
617 CLOUTIER, J. K., MCMANN, C. L., ODERBERG, I. M. & REDDIEN, P. W. 2021. activin-2 is
618 required for regeneration of polarity on the planarian anterior-posterior axis. *PLoS Genet,*
619 17**,** e1009466.
620 COLAVITA, A. & CULOTTI, J. G. 1998. Suppressors of ectopic UNC-5 growth cone steering
621 identify eight genes involved in axon guidance in Caenorhabditis elegans. *Dev Biol,* 194**,**
622 72-85.
623 CURRIE, K. W. & PEARSON, B. J. 2013. Transcription factors lhx1/5-1 and pitx are required
624 for the maintenance and regeneration of serotonergic neurons in planarians. *Development,*
625 140**,** 3577-88.
626 DALVIN, S., ANSELMO, M. A., PRODHAN, P., KOMATSUZAKI, K., SCHNITZER, J. J. &
627 KINANE, T. B. 2003. Expression of Netrin-1 and its two receptors DCC and UNC5H2 in
628 the developing mouse lung. *Gene Expr Patterns,* 3**,** 279-83.
629 DE BREUCK, S., LARDON, J., ROOMAN, I. & BOUWENS, L. 2003. Netrin-1 expression in
630 fetal and regenerating rat pancreas and its effect on the migration of human pancreatic
631 duct and porcine islet precursor cells. *Diabetologia,* 46**,** 926-33.
632 FAZELI, A., DICKINSON, S. L., HERMISTON, M. L., TIGHE, R. V., STEEN, R. G., SMALL,
633 C. G., STOECKLI, E. T., KEINO-MASU, K., MASU, M., RAYBURN, H., SIMONS, J.,
634 BRONSON, R. T., GORDON, J. I., TESSIER-LAVIGNE, M. & WEINBERG, R. A.
635 1997. Phenotype of mice lacking functional Deleted in colorectal cancer (Dcc) gene.
636 *Nature,* 386**,** 796-804.

FINCHER, C. T., WURTZEL, O., DE HOOG, T., KRAVARIK, K. M. & REDDIEN, P. W. 2018. Cell type transcriptome atlas for the planarian Schmidtea mediterranea. *Science,* 360.

FINCI, L. I., KRUGER, N., SUN, X., ZHANG, J., CHEGKAZI, M., WU, Y., SCHENK, G., MERTENS, H. D. T., SVERGUN, D. I., ZHANG, Y., WANG, J. H. & MEIJERS, R. 2014. The crystal structure of netrin-1 in complex with DCC reveals the bifunctionality of netrin-1 as a guidance cue. *Neuron,* 83**,** 839-849.

GAVINO, M. A. & REDDIEN, P. W. 2011. A Bmp/Admp regulatory circuit controls maintenance and regeneration of dorsal-ventral polarity in planarians. *Curr Biol,* 21**,** 294-9.

GAVINO, M. A., WENEMOSER, D., WANG, I. E. & REDDIEN, P. W. 2013. Tissue absence initiates regeneration through follistatin-mediated inhibition of activin signaling. *Elife,* 2**,** e00247.

GLISE, B., MILLER, C. A., CROZATIER, M., HALBISEN, M. A., WISE, S., OLSON, D. J., VINCENT, A. & BLAIR, S. S. 2005. Shifted, the Drosophila ortholog of Wnt inhibitory factor-1, controls the distribution and movement of Hedgehog. *Dev Cell,* 8**,** 255-66.

GURLEY, K. A., ELLIOTT, S. A., SIMAKOV, O., SCHMIDT, H. A., HOLSTEIN, T. W. & SANCHEZ ALVARADO, A. 2010. Expression of secreted Wnt pathway components reveals unexpected complexity of the planarian amputation response. *Dev Biol,* 347**,** 24-39.

GURLEY, K. A., RINK, J. C. & SANCHEZ ALVARADO, A. 2008. Beta-catenin defines head versus tail identity during planarian regeneration and homeostasis. *Science,* 319**,** 323-7.

HAMELIN, M., ZHOU, Y., SU, M. W., SCOTT, I. M. & CULOTTI, J. G. 1993. Expression of the UNC-5 guidance receptor in the touch neurons of C. elegans steers their axons dorsally. *Nature,* 364**,** 327-30.

HARRIS, R., SABATELLI, L. M. & SEEGER, M. A. 1996. Guidance cues at the Drosophila CNS midline: identification and characterization of two Drosophila Netrin/UNC-6 homologs. *Neuron,* 17**,** 217-28.

HAYASHI, T., MOTOISHI, M., YAZAWA, S., ITOMI, K., TANEGASHIMA, C., NISHIMURA, O., AGATA, K. & TARUI, H. 2011. A LIM-homeobox gene is required for differentiation of Wnt-expressing cells at the posterior end of the planarian body. *Development,* 138**,** 3679-88.

HEDGECOCK, E. M., CULOTTI, J. G. & HALL, D. H. 1990. The unc-5, unc-6, and unc-40 genes guide circumferential migrations of pioneer axons and mesodermal cells on the epidermis in C. elegans. *Neuron,* 4**,** 61-85.

HONG, K., HINCK, L., NISHIYAMA, M., POO, M. M., TESSIER-LAVIGNE, M. & STEIN, E. 1999. A ligand-gated association between cytoplasmic domains of UNC5 and DCC family receptors converts netrin-induced growth cone attraction to repulsion. *Cell,* 97**,** 927-41.

HSIEH, J. C., KODJABACHIAN, L., REBBERT, M. L., RATTNER, A., SMALLWOOD, P. M., SAMOS, C. H., NUSSE, R., DAWID, I. B. & NATHANS, J. 1999. A new secreted protein that binds to Wnt proteins and inhibits their activities. *Nature,* 398**,** 431-6.

IGLESIAS, M., GOMEZ-SKARMETA, J. L., SALO, E. & ADELL, T. 2008. Silencing of Smed-betacatenin1 generates radial-like hypercephalized planarians. *Development,* 135**,** 1215-21.

ISHII, N., WADSWORTH, W. G., STERN, B. D., CULOTTI, J. G. & HEDGECOCK, E. M. 1992. UNC-6, a laminin-related protein, guides cell and pioneer axon migrations in C. elegans. *Neuron,* 9**,** 873-81.

KANG, J. S., YI, M. J., ZHANG, W., FEINLEIB, J. L., COLE, F. & KRAUSS, R. S. 2004. Netrins and neogenin promote myotube formation. *J Cell Biol,* 167**,** 493-504.

KEINO-MASU, K., MASU, M., HINCK, L., LEONARDO, E. D., CHAN, S. S., CULOTTI, J. G. & TESSIER-LAVIGNE, M. 1996. Deleted in Colorectal Cancer (DCC) encodes a netrin receptor. *Cell,* 87**,** 175-85.

KELEMAN, K. & DICKSON, B. J. 2001. Short- and long-range repulsion by the Drosophila Unc5 netrin receptor. *Neuron,* 32**,** 605-17.

KENNEDY, T. E., SERAFINI, T., DE LA TORRE, J. R. & TESSIER-LAVIGNE, M. 1994. Netrins are diffusible chemotropic factors for commissural axons in the embryonic spinal cord. *Cell,* 78**,** 425-35.

KHARCHENKO, P. V., SILBERSTEIN, L. & SCADDEN, D. T. 2014. Bayesian approach to single-cell differential expression analysis. *Nat Methods,* 11**,** 740-2.

KING, R. S. & NEWMARK, P. A. 2013. In situ hybridization protocol for enhanced detection of gene expression in the planarian Schmidtea mediterranea. *BMC Dev Biol,* 13**,** 8.

KOLODZIEJ, P. A., TIMPE, L. C., MITCHELL, K. J., FRIED, S. R., GOODMAN, C. S., JAN, L. Y. & JAN, Y. N. 1996. frazzled encodes a Drosophila member of the DCC immunoglobulin subfamily and is required for CNS and motor axon guidance. *Cell,* 87**,** 197-204.

LAI WING SUN, K., CORREIA, J. P. & KENNEDY, T. E. 2011. Netrins: versatile extracellular cues with diverse functions. *Development,* 138**,** 2153-69.

LANDER, R. & PETERSEN, C. P. 2016. Wnt, Ptk7, and FGFRL expression gradients control trunk positional identity in planarian regeneration. *Elife,* 5.

LI, D. J., MCMANN, C. L. & REDDIEN, P. W. 2019. Nuclear receptor NR4A is required for patterning at the ends of the planarian anterior-posterior axis. *Elife,* 8.

LIU, Y., STEIN, E., OLIVER, T., LI, Y., BRUNKEN, W. J., KOCH, M., TESSIER-LAVIGNE, M. & HOGAN, B. L. 2004. Novel role for Netrins in regulating epithelial behavior during lung branching morphogenesis. *Curr Biol,* 14**,** 897-905.

LLAMBI, F., CAUSERET, F., BLOCH-GALLEGO, E. & MEHLEN, P. 2001. Netrin-1 acts as a survival factor via its receptors UNC5H and DCC. *EMBO J,* 20**,** 2715-22.

LOWE, C. J., TERASAKI, M., WU, M., FREEMAN, R. M., JR., RUNFT, L., KWAN, K., HAIGO, S., ARONOWICZ, J., LANDER, E., GRUBER, C., SMITH, M., KIRSCHNER, M. & GERHART, J. 2006. Dorsoventral patterning in hemichordates: insights into early chordate evolution. *PLoS Biol,* 4**,** e291.

MÄRZ, M., SEEBECK, F. & BARTSCHERER, K. 2013. A Pitx transcription factor controls the establishment and maintenance of the serotonergic lineage in planarians. *Development,* 140**,** 4499-4509.

MEHLEN, P., RABIZADEH, S., SNIPAS, S. J., ASSA-MUNT, N., SALVESEN, G. S. & BREDESEN, D. E. 1998. The DCC gene product induces apoptosis by a mechanism requiring receptor proteolysis. *Nature,* 395**,** 801-4.

MITCHELL, K. J., DOYLE, J. L., SERAFINI, T., KENNEDY, T. E., TESSIER-LAVIGNE, M., GOODMAN, C. S. & DICKSON, B. J. 1996. Genetic analysis of Netrin genes in Drosophila: Netrins guide CNS commissural axons and peripheral motor axons. *Neuron,* 17**,** 203-15.

728 MOLINA, M. D., SALO, E. & CEBRIA, F. 2007. The BMP pathway is essential for re-
729 specification and maintenance of the dorsoventral axis in regenerating and intact
730 planarians. *Dev Biol,* 311**,** 79-94.
731 ODERBERG, I. M., LI, D. J., SCIMONE, M. L., GAVINO, M. A. & REDDIEN, P. W. 2017.
732 Landmarks in Existing Tissue at Wounds Are Utilized to Generate Pattern in
733 Regenerating Tissue. *Curr Biol,* 27**,** 733-742.
734 ONICHTCHOUK, D., CHEN, Y. G., DOSCH, R., GAWANTKA, V., DELIUS, H.,
735 MASSAGUE, J. & NIEHRS, C. 1999. Silencing of TGF-beta signalling by the
736 pseudoreceptor BAMBI. *Nature,* 401**,** 480-5.
737 ORII, H. & WATANABE, K. 2007. Bone morphogenetic protein is required for dorso-ventral
738 patterning in the planarian Dugesia japonica. *Dev Growth Differ,* 49**,** 345-9.
739 ORII, H. K., K; AGATA, K; WATANABE, K 1998. Molecular Cloning of the Bone
740 Morphogenetic Protein (BMP) Gene from the Planarian Dugesia japonica. *Zoolog Sci,*
741 15**,** 6.
742 OWEN, J. H., WAGNER, D. E., CHEN, C. C., PETERSEN, C. P. & REDDIEN, P. W. 2015.
743 teashirt is required for head-versus-tail regeneration polarity in planarians. *Development,*
744 142**,** 1062-72.
745 PEARSON, B. J., EISENHOFFER, G. T., GURLEY, K. A., RINK, J. C., MILLER, D. E. &
746 SANCHEZ ALVARADO, A. 2009. Formaldehyde-based whole-mount in situ
747 hybridization method for planarians. *Dev Dyn,* 238**,** 443-50.
748 PETERSEN, C. P. & REDDIEN, P. W. 2008. Smed-betacatenin-1 is required for anteroposterior
749 blastema polarity in planarian regeneration. *Science,* 319**,** 327-30.
750 PETERSEN, C. P. & REDDIEN, P. W. 2009. A wound-induced Wnt expression program
751 controls planarian regeneration polarity. *Proc Natl Acad Sci U S A,* 106**,** 17061-6.
752 PETERSEN, C. P. & REDDIEN, P. W. 2011. Polarized notum activation at wounds inhibits Wnt
753 function to promote planarian head regeneration. *Science,* 332**,** 852-5.
754 RAZ, A. A., SRIVASTAVA, M., SALVAMOSER, R. & REDDIEN, P. W. 2017. Acoel
755 regeneration mechanisms indicate an ancient role for muscle in regenerative patterning.
756 *Nat Commun,* 8**,** 1260.
757 REDDIEN, P. W. 2018. The Cellular and Molecular Basis for Planarian Regeneration. *Cell,* 175**,**
758 327-345.
759 REDDIEN, P. W., BERMANGE, A. L., KICZA, A. M. & SANCHEZ ALVARADO, A. 2007.
760 BMP signaling regulates the dorsal planarian midline and is needed for asymmetric
761 regeneration. *Development,* 134**,** 4043-51.
762 REUTER, H., MARZ, M., VOGG, M. C., ECCLES, D., GRIFOL-BOLDU, L., WEHNER, D.,
763 OWLARN, S., ADELL, T., WEIDINGER, G. & BARTSCHERER, K. 2015. Beta-
764 catenin-dependent control of positional information along the AP body axis in planarians
765 involves a teashirt family member. *Cell Rep,* 10**,** 253-65.
766 ROBERTS-GALBRAITH, R. H. & NEWMARK, P. A. 2013. Follistatin antagonizes activin
767 signaling and acts with notum to direct planarian head regeneration. *Proc Natl Acad Sci*
768 *U S A,* 110**,** 1363-8.
769 ROSS, K. G., OMURO, K. C., TAYLOR, M. R., MUNDAY, R. K., HUBERT, A., KING, R. S.
770 & ZAYAS, R. M. 2015. Novel monoclonal antibodies to study tissue regeneration in
771 planarians. *BMC Dev Biol,* 15**,** 2.
772 ROUHANA, L., WEISS, J. A., FORSTHOEFEL, D. J., LEE, H., KING, R. S., INOUE, T.,
773 SHIBATA, N., AGATA, K. & NEWMARK, P. A. 2013. RNA interference by feeding in

774 vitro-synthesized double-stranded RNA to planarians: methodology and dynamics. *Dev*
775 *Dyn,* 242**,** 718-30.
776 SCHAD, E. G. & PETERSEN, C. P. 2020. STRIPAK Limits Stem Cell Differentiation of a
777 WNT Signaling Center to Control Planarian Axis Scaling. *Curr Biol,* 30**,** 254-263 e2.
778 SCIMONE, M. L., ATABAY, K. D., FINCHER, C. T., BONNEAU, A. R., LI, D. J. &
779 REDDIEN, P. W. 2020. Muscle and neuronal guidepost-like cells facilitate planarian
780 visual system regeneration. *Science,* 368.
781 SCIMONE, M. L., COTE, L. E. & REDDIEN, P. W. 2017. Orthogonal muscle fibres have
782 different instructive roles in planarian regeneration. *Nature,* 551**,** 623-628.
783 SCIMONE, M. L., COTE, L. E., ROGERS, T. & REDDIEN, P. W. 2016. Two FGFRL-Wnt
784 circuits organize the planarian anteroposterior axis. *Elife,* 5.
785 SCIMONE, M. L., WURTZEL, O., MALECEK, K., FINCHER, C. T., ODERBERG, I. M.,
786 KRAVARIK, K. M. & REDDIEN, P. W. 2018. foxF-1 Controls Specification of Non-
787 body Wall Muscle and Phagocytic Cells in Planarians. *Curr Biol,* 28**,** 3787-3801 e6.
788 SERAFINI, T., KENNEDY, T. E., GALKO, M. J., MIRZAYAN, C., JESSELL, T. M. &
789 TESSIER-LAVIGNE, M. 1994. The netrins define a family of axon outgrowth-
790 promoting proteins homologous to C. elegans UNC-6. *Cell,* 78**,** 409-24.
791 SRINIVASAN, K., STRICKLAND, P., VALDES, A., SHIN, G. C. & HINCK, L. 2003. Netrin-
792 1/neogenin interaction stabilizes multipotent progenitor cap cells during mammary gland
793 morphogenesis. *Dev Cell,* 4**,** 371-82.
794 SRIVASTAVA, M. 2022. Studying development, regeneration, stem cells, and more in the acoel
795 Hofstenia miamia. *Curr Top Dev Biol,* 147**,** 153-172.
796 SRIVASTAVA, M., MAZZA-CURLL, K. L., VAN WOLFSWINKEL, J. C. & REDDIEN, P.
797 W. 2014. Whole-body acoel regeneration is controlled by Wnt and Bmp-Admp signaling.
798 *Curr Biol,* 24**,** 1107-13.
799 STUCKEMANN, T., CLELAND, J. P., WERNER, S., THI-KIM VU, H., BAYERSDORF, R.,
800 LIU, S. Y., FRIEDRICH, B., JULICHER, F. & RINK, J. C. 2017. Antagonistic Self-
801 Organizing Patterning Systems Control Maintenance and Regeneration of the
802 Anteroposterior Axis in Planarians. *Dev Cell,* 40**,** 248-263 e4.
803 TEWARI, A. G., STERN, S. R., ODERBERG, I. M. & REDDIEN, P. W. 2018. Cellular and
804 Molecular Responses Unique to Major Injury Are Dispensable for Planarian
805 Regeneration. *Cell Rep,* 25**,** 2577-2590 e3.
806 VOGG, M. C., GALLIOT, B. & TSIAIRIS, C. D. 2019. Model systems for regeneration: Hydra.
807 *Development,* 146.
808 VU, H. T., MANSOUR, S., KUCKEN, M., BLASSE, C., BASQUIN, C., AZIMZADEH, J.,
809 MYERS, E. W., BRUSCH, L. & RINK, J. C. 2019. Dynamic Polarization of the
810 Multiciliated Planarian Epidermis between Body Plan Landmarks. *Dev Cell,* 51**,** 526-542
811 e6.
812 WAGNER, D. E., WANG, I. E. & REDDIEN, P. W. 2011. Clonogenic neoblasts are pluripotent
813 adult stem cells that underlie planarian regeneration. *Science,* 332**,** 811-6.
814 WITCHLEY, J. N., MAYER, M., WAGNER, D. E., OWEN, J. H. & REDDIEN, P. W. 2013.
815 Muscle cells provide instructions for planarian regeneration. *Cell Rep,* 4**,** 633-41.
816 YEBRA, M., MONTGOMERY, A. M., DIAFERIA, G. R., KAIDO, T., SILLETTI, S., PEREZ,
817 B., JUST, M. L., HILDBRAND, S., HURFORD, R., FLORKIEWICZ, E., TESSIER-
818 LAVIGNE, M. & CIRULLI, V. 2003. Recognition of the neural chemoattractant Netrin-1

819 by integrins alpha6beta4 and alpha3beta1 regulates epithelial cell adhesion and
820 migration. *Dev Cell,* 5**,** 695-707.
821 ZENG, A., LI, H., GUO, L., GAO, X., MCKINNEY, S., WANG, Y., YU, Z., PARK, J.,
822 SEMERAD, C., ROSS, E., CHENG, L. C., DAVIES, E., LEI, K., WANG, W., PERERA,
823 A., HALL, K., PEAK, A., BOX, A. & SANCHEZ ALVARADO, A. 2018. Prospectively
824 Isolated Tetraspanin(+) Neoblasts Are Adult Pluripotent Stem Cells Underlying Planaria
825 Regeneration. *Cell,* 173**,** 1593-1608 e20.
826
827
828

Figure 1

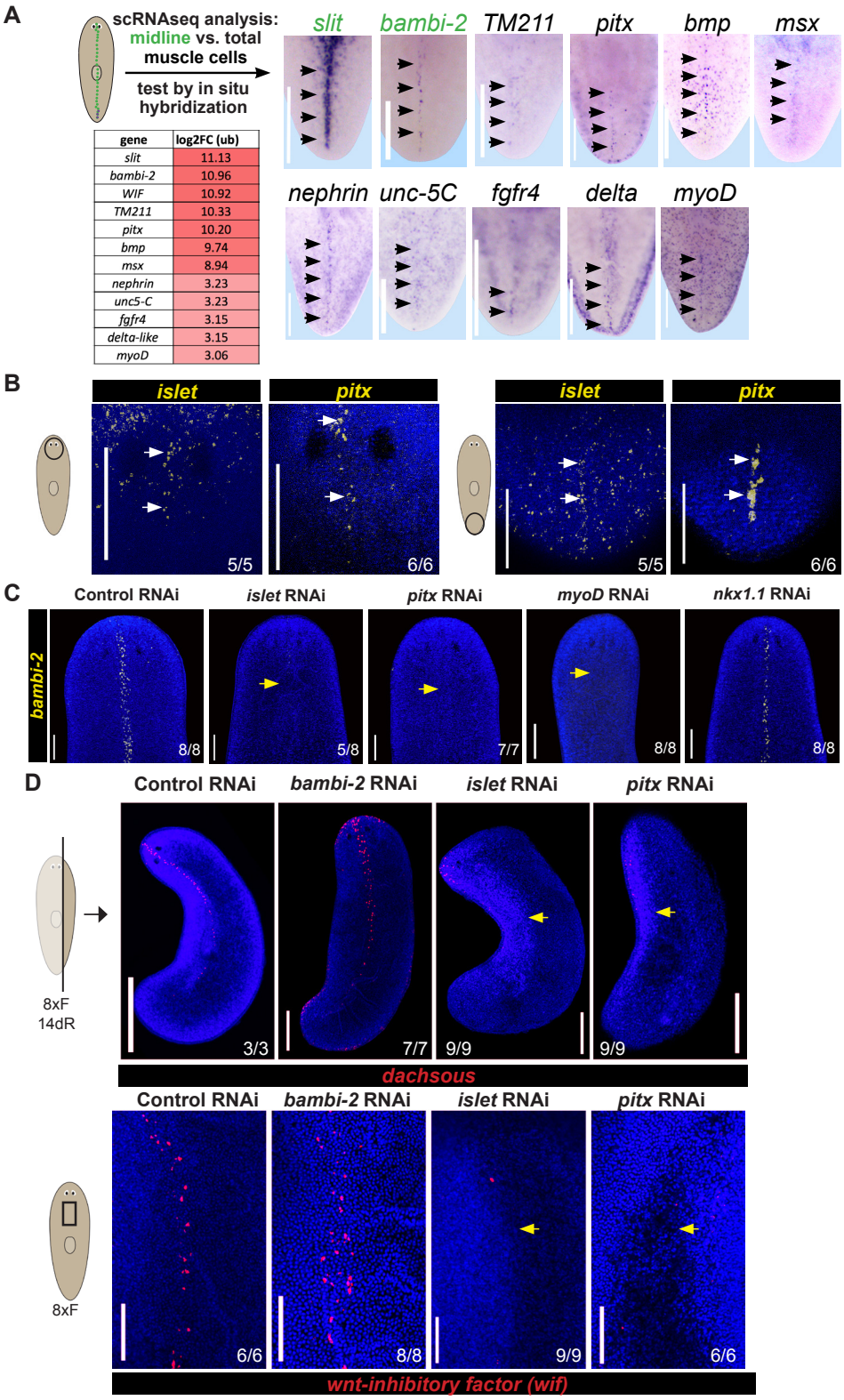

gene	log2FC (ub)
slit	11.13
bambi-2	10.96
WIF	10.92
TM211	10.33
pitx	10.20
bmp	9.74
msx	8.94
nephrin	3.23
unc5-C	3.23
fgfr4	3.15
delta-like	3.15
myoD	3.06

Figure 2

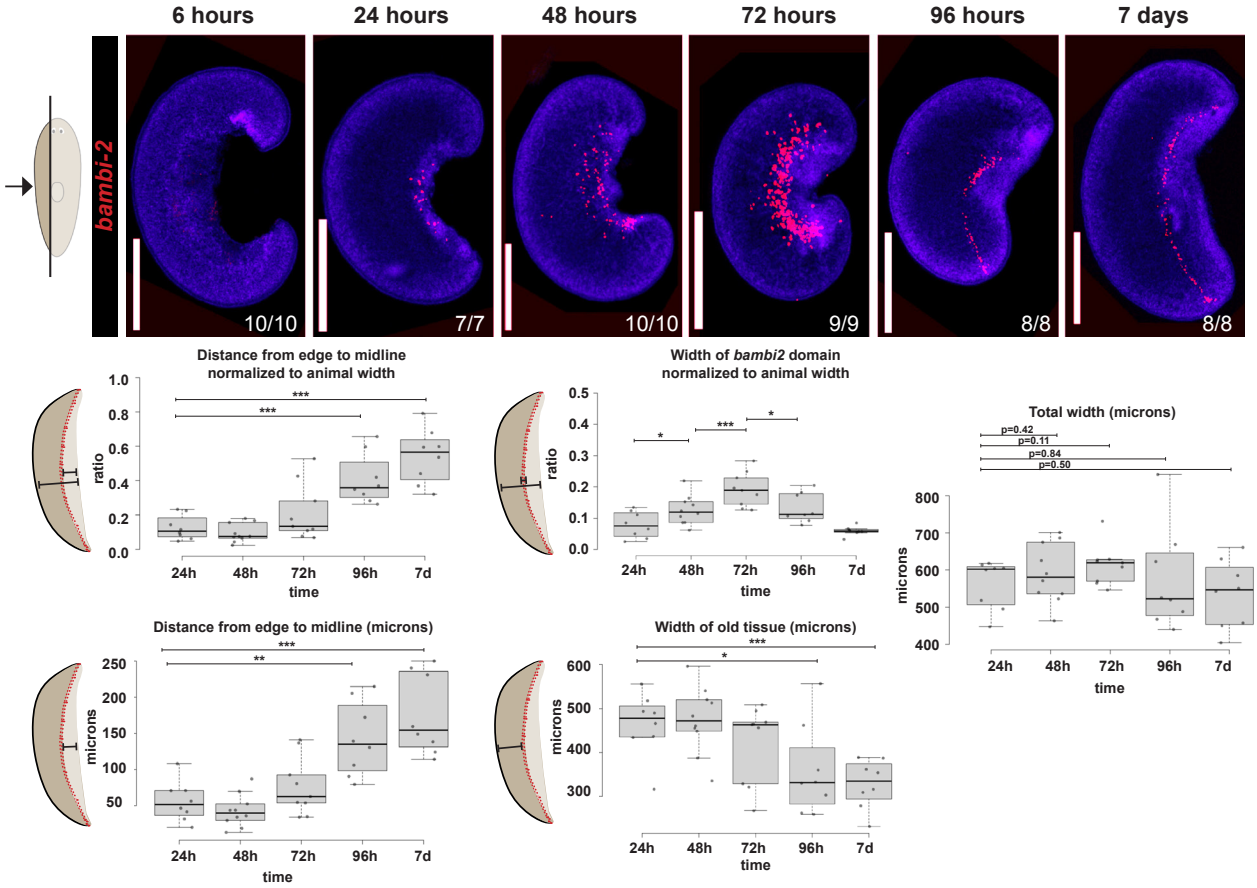
6 hours
24 hours
48 hours
72 hours
96 hours
7 days
bambi-2
10/10
7/7
10/10
9/9
8/8
8/8
Distance from edge to midline normalized to animal width
ratio
time
Width of bambi2 domain normalized to animal width
ratio
time
Total width (microns)
p=0.42
p=0.11
p=0.84
p=0.50
microns
time
Distance from edge to midline (microns)
microns
time
Width of old tissue (microns)
microns
time
24h
48h
72h
96h
7d

Figure 3

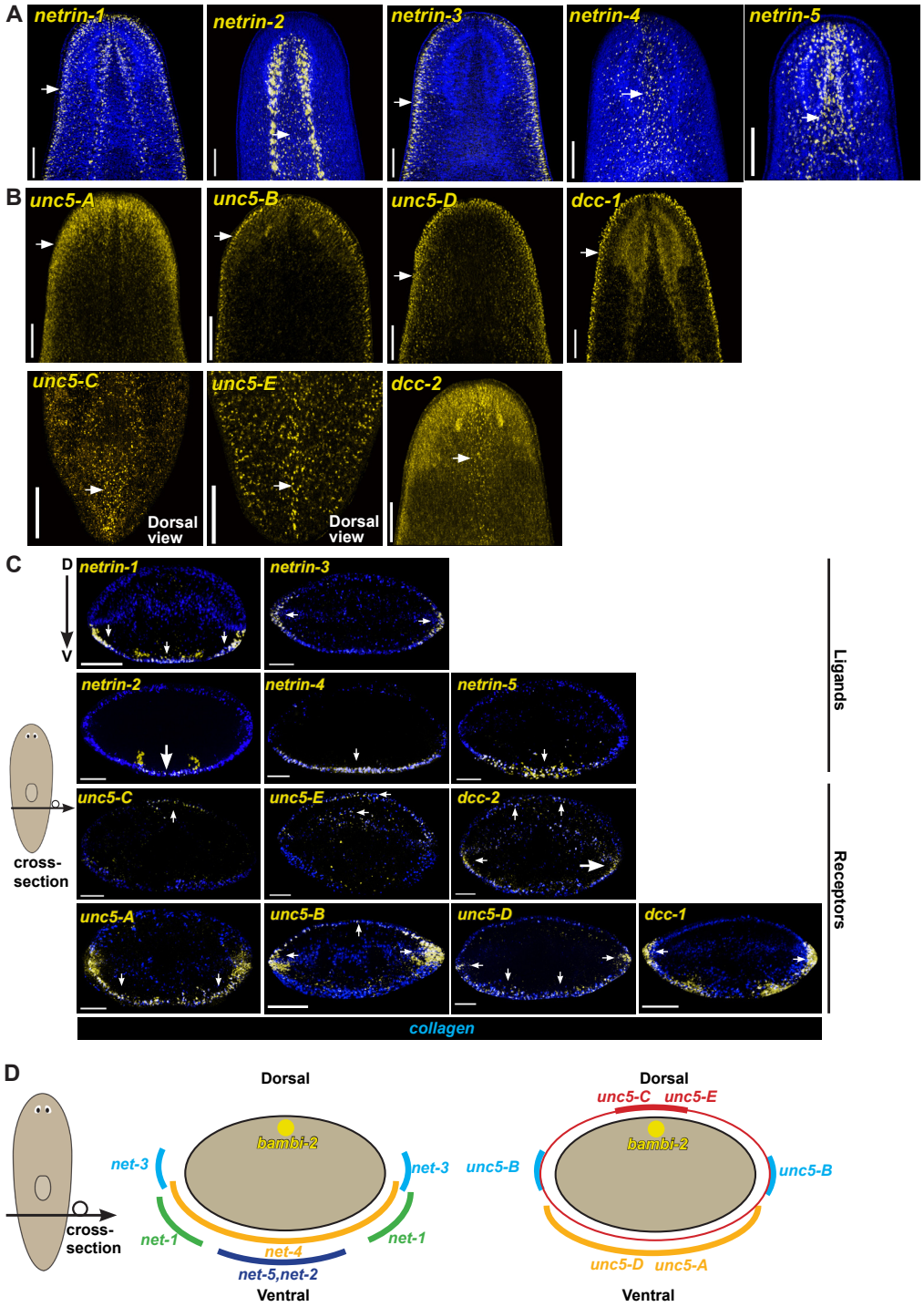
A
netrin-1
netrin-2
netrin-3
netrin-4
netrin-5
B
unc5-A
unc5-B
unc5-D
dcc-1
unc5-C
unc5-E
dcc-2
Dorsal view
Dorsal view
C
D
V
netrin-1
netrin-3
netrin-2
netrin-4
netrin-5
Ligands
cross-section
unc5-C
unc5-E
dcc-2
unc5-A
unc5-B
unc5-D
dcc-1
Receptors
collagen
D
cross-section
Dorsal
bambi-2
net-3
net-3
net-1
net-1
net-4
net-5,net-2
Ventral
Dorsal
unc5-C
unc5-E
bambi-2
unc5-B
unc5-B
unc5-D
unc5-A
Ventral

Figure 4

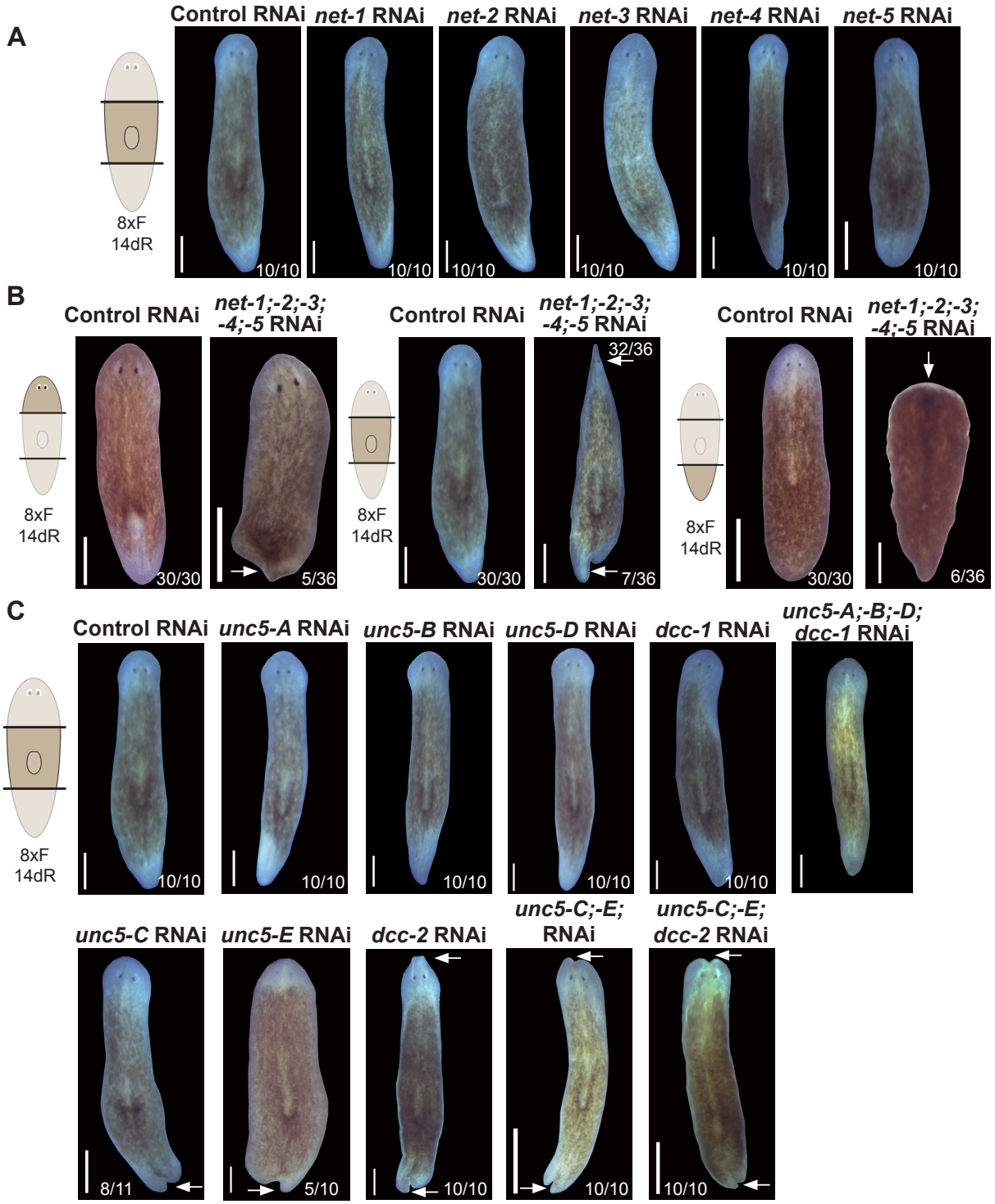
A
Control RNAi
net-1 RNAi
net-2 RNAi
net-3 RNAi
net-4 RNAi
net-5 RNAi
8xF
14dR
10/10
10/10
10/10
10/10
10/10
10/10
B
Control RNAi
net-1;-2;-3;
-4;-5 RNAi
8xF
14dR
30/30
5/36
Control RNAi
net-1;-2;-3;
-4;-5 RNAi
32/36
8xF
14dR
30/30
7/36
Control RNAi
net-1;-2;-3;
-4;-5 RNAi
8xF
14dR
30/30
6/36
C
Control RNAi
unc5-A RNAi
unc5-B RNAi
unc5-D RNAi
dcc-1 RNAi
unc5-A;-B;-D;
dcc-1 RNAi
8xF
14dR
10/10
10/10
10/10
10/10
10/10
unc5-C RNAi
unc5-E RNAi
dcc-2 RNAi
unc5-C;-E;
RNAi
unc5-C;-E;
dcc-2 RNAi
8/11
5/10
10/10
10/10
10/10

Figure 5

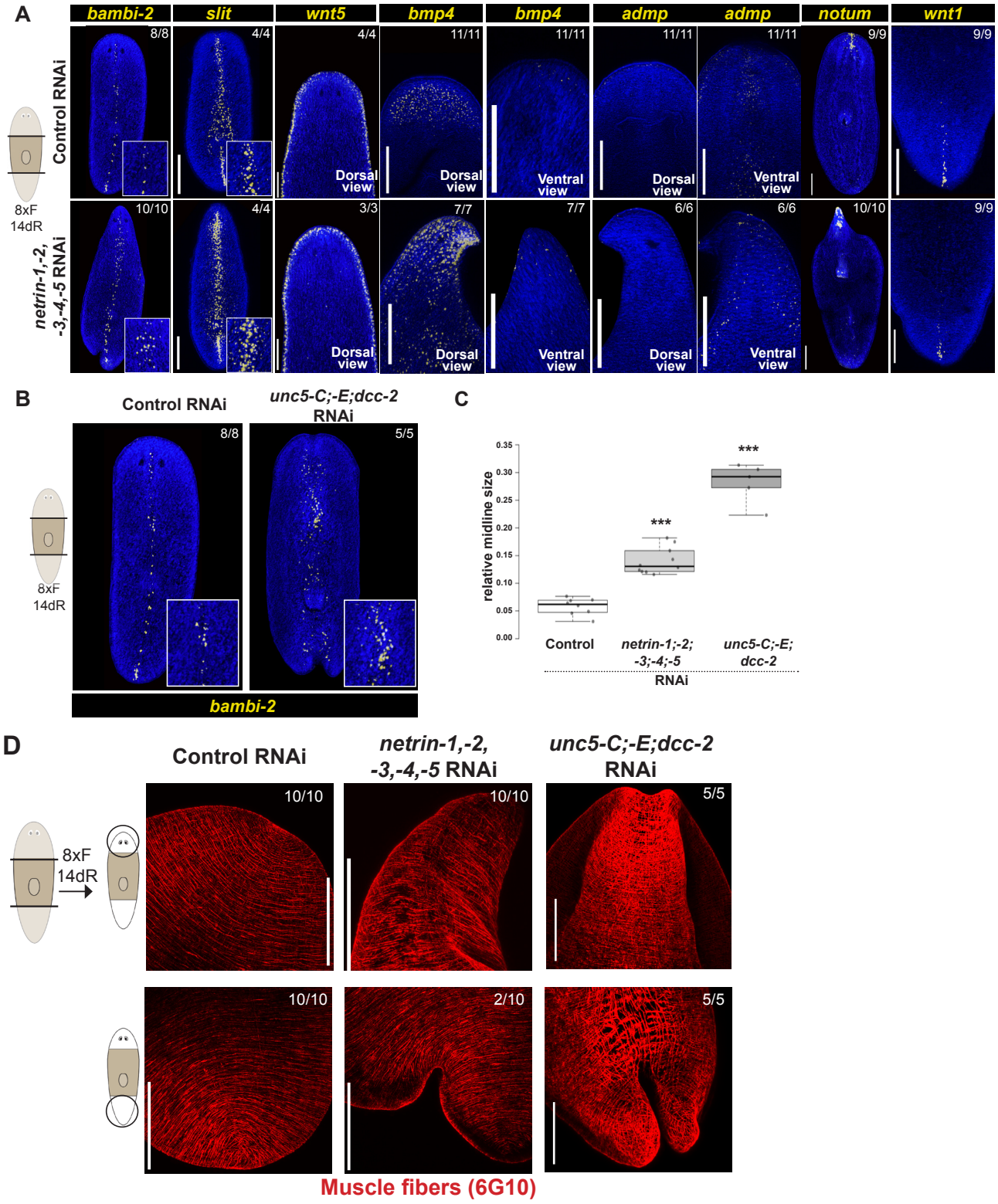
A
bambi-2
slit
wnt5
bmp4
bmp4
admp
admp
notum
wnt1
Control RNAi
netrin-1,-2, -3,-4,-5 RNAi
8xF
14dR
8/8
4/4
4/4
11/11
11/11
11/11
11/11
9/9
9/9
10/10
4/4
3/3
7/7
7/7
6/6
6/6
10/10
9/9
Dorsal view
Ventral view
B
Control RNAi
unc5-C;-E;dcc-2 RNAi
8/8
5/5
bambi-2
C
relative midline size
0.35
0.30
0.25
0.20
0.15
0.10
0.05
0.00
***
***
Control
netrin-1;-2; -3;-4;-5
unc5-C;-E; dcc-2
RNAi
D
Control RNAi
netrin-1,-2, -3,-4,-5 RNAi
unc5-C;-E;dcc-2 RNAi
10/10
10/10
5/5
10/10
2/10
5/5
Muscle fibers (6G10)

Figure 6

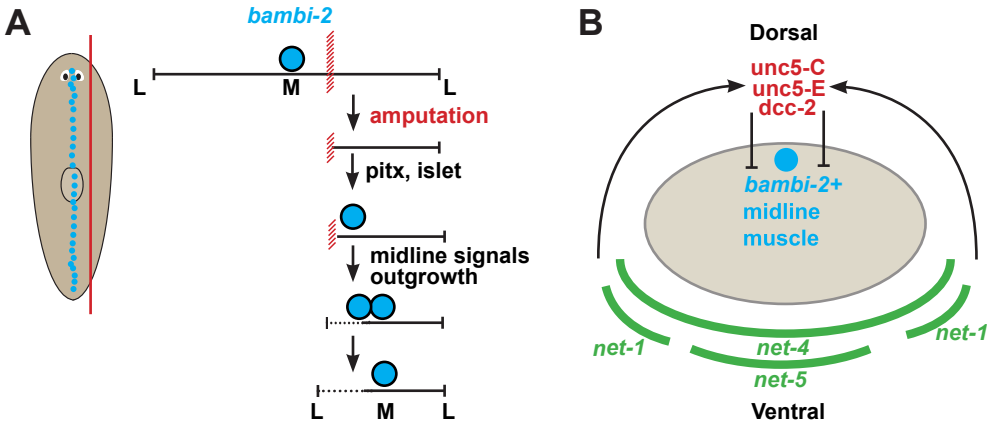
A
bambi-2
L
M
L
amputation
pitx, islet
midline signals
outgrowth
L
M
L
B
Dorsal
unc5-C
unc5-E
dcc-2
bambi-2+
midline
muscle
net-1
net-4
net-1
net-5
Ventral

Figure S1

A

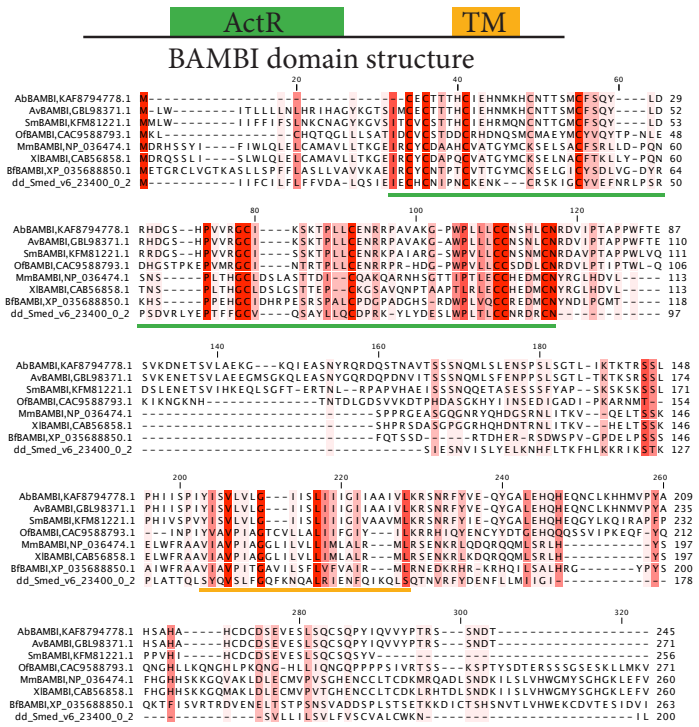
ActR
TM
BAMBI domain structure
AbBAMBI,KAF8794778.1
AvBAMBI,GBL98371.1
SmBAMBI,KFM81221.1
OfBAMBI,CAC9588793.1
MmBAMBI,NP_036474.1
XlBAMBI,CAB56858.1
BfBAMBI,XP_035688850.1
dd_Smed_v6_23400_0_2

B

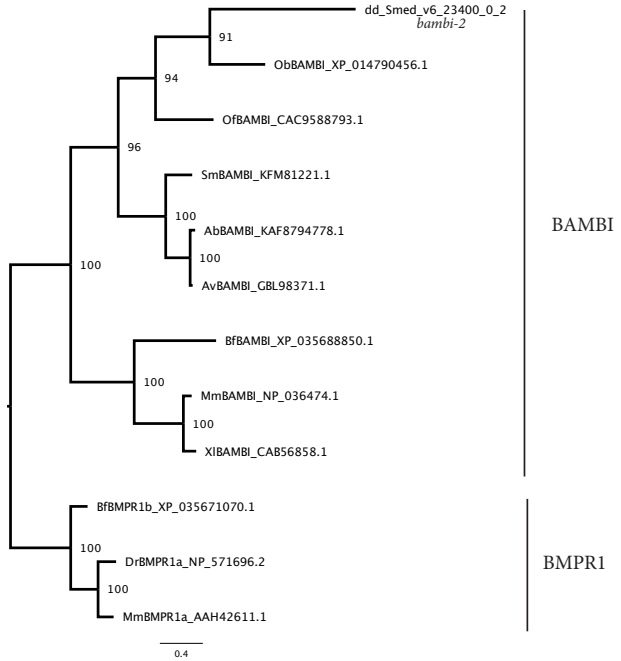
dd_Smed_v6_23400_0_2
bambi-2
ObBAMBI_XP_014790456.1
OfBAMBI_CAC9588793.1
SmBAMBI_KFM81221.1
AbBAMBI_KAF8794778.1
AvBAMBI_GBL98371.1
BfBAMBI_XP_035688850.1
MmBAMBI_NP_036474.1
XlBAMBI_CAB56858.1
BfBMPR1b_XP_035671070.1
DrBMPR1a_NP_571696.2
MmBMPR1a_AAH42611.1
BAMBI
BMPR1
0.4

Figure S2

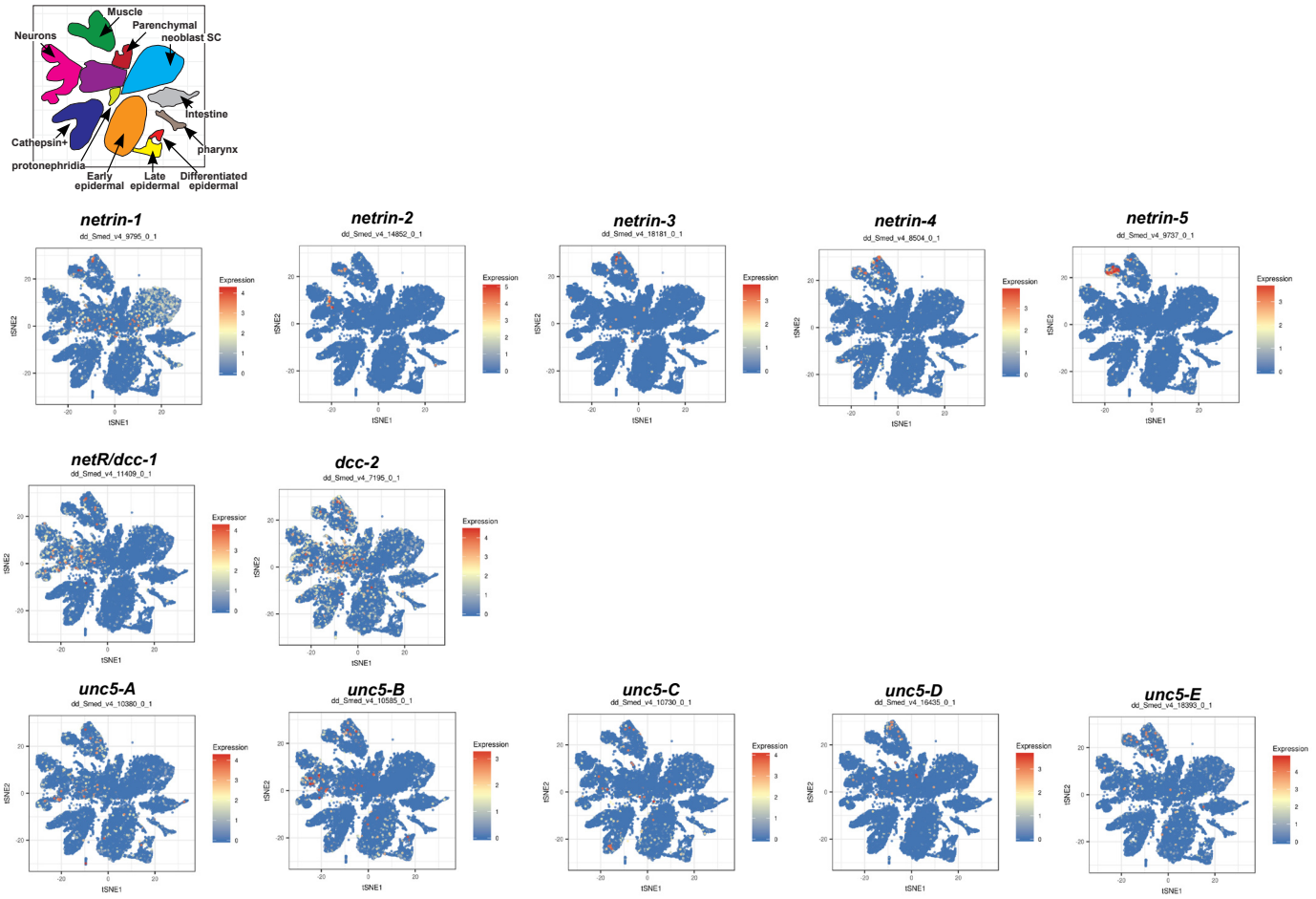
Muscle
Parenchymal
Neurons
neoblast SC
Intestine
Cathepsin+
pharynx
protonephridia
Early epidermal
Late epidermal
Differentiated epidermal
netrin-1
dd_Smed_v4_9795_0_1
netrin-2
dd_Smed_v4_14852_0_1
netrin-3
dd_Smed_v4_18181_0_1
netrin-4
dd_Smed_v4_8504_0_1
netrin-5
dd_Smed_v4_9737_0_1
netR/dcc-1
dd_Smed_v4_11409_0_1
dcc-2
dd_Smed_v4_7195_0_1
unc5-A
dd_Smed_v4_10380_0_1
unc5-B
dd_Smed_v4_10585_0_1
unc5-C
dd_Smed_v4_10730_0_1
unc5-D
dd_Smed_v4_16435_0_1
unc5-E
dd_Smed_v4_18393_0_1
Expression
tSNE1
tSNE2

Figure S3

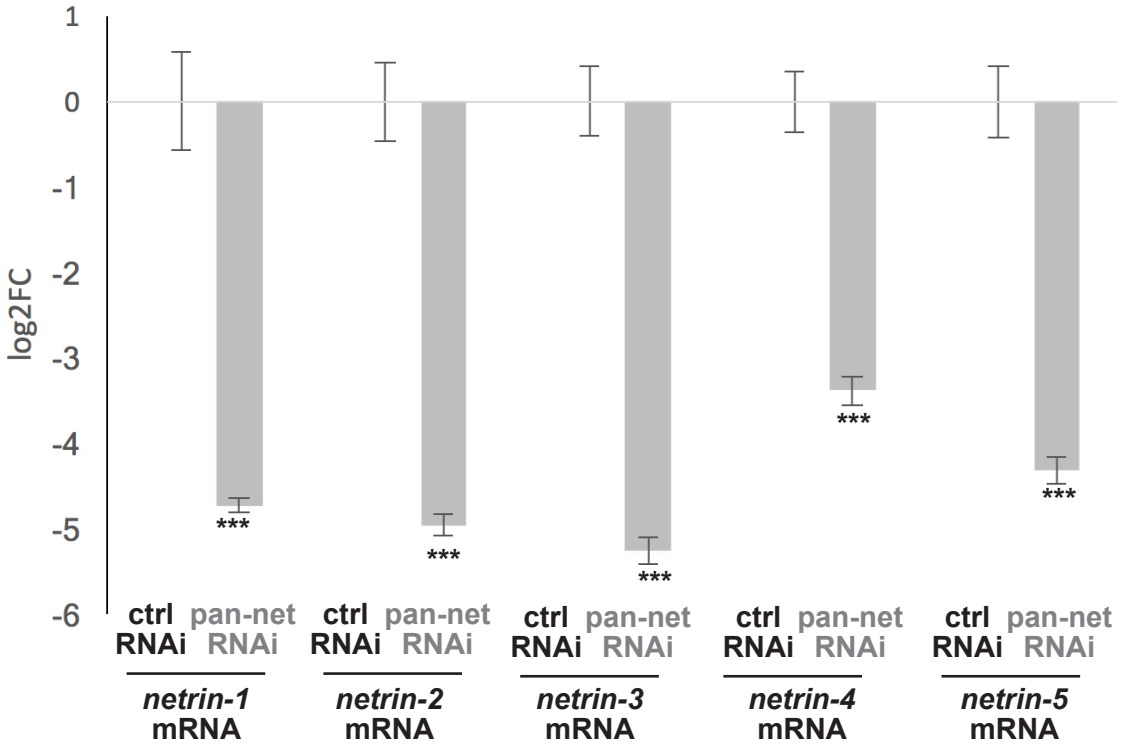
1
0
-1
-2
-3
-4
-5
-6
log2FC
***
***
***
***
***
ctrl RNAi
pan-net RNAi
netrin-1 mRNA
netrin-2 mRNA
netrin-3 mRNA
netrin-4 mRNA
netrin-5 mRNA

Figure S4

A

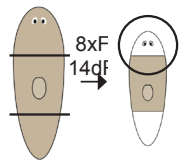

Score for pointy blastema

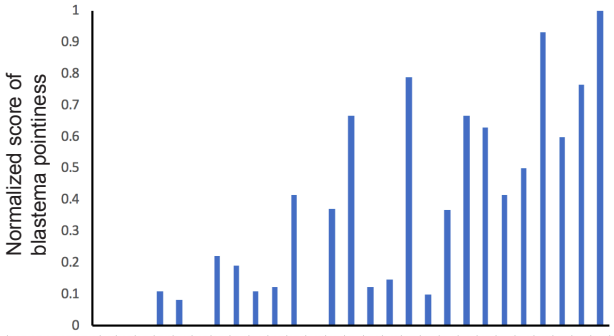

netrin-1	-	+	+	+	+	-	-	-	-	-	-	+	+	+	+	+	+	-	-	-	-	+	+	+	+	-	+
netrin-2	-	+	-	-	-	-	+	+	+	-	-	-	+	+	+	-	-	-	+	+	+	-	+	+	+	-	+	+
netrin-3	-	-	+	-	-	-	+	-	-	+	+	-	+	-	-	+	+	-	+	+	-	+	+	+	-	+	+	+
netrin-4	-	-	-	+	-	-	+	-	+	-	+	-	+	-	+	-	+	+	-	+	-	+	+	+	-	+	+	+
netrin-5	-	-	-	-	-	+	-	-	+	-	+	+	-	-	+	-	+	+	-	+	+	+	-	+	+	+	+	+

RNAi condition

8xF
14dR

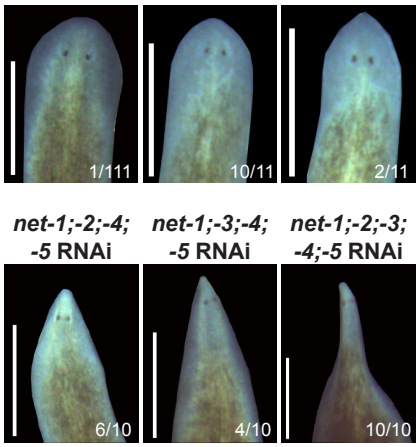

B

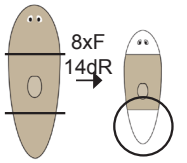

Score for indented blastema

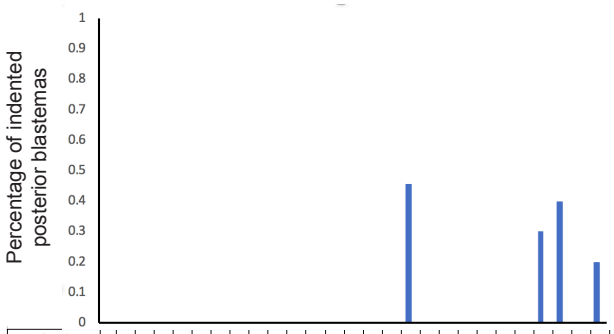

netrin-1	-	+	+	+	+	-	-	-	-	-	-	+	+	+	+	+	+	-	-	-	-	+	+	+	+	-	+
netrin-2	-	+	-	-	-	-	+	+	+	-	-	-	+	+	+	-	-	-	+	+	+	-	+	+	+	-	+	+
netrin-3	-	-	+	-	-	+	-	-	+	+	-	+	-	-	+	+	-	+	+	+	-	+	+	+	-	+	+	+
netrin-4	-	-	-	+	-	-	+	-	+	-	+	-	+	-	+	-	+	+	-	+	+	+	-	+	+	+	+	+
netrin-5	-	-	-	-	+	-	-	+	-	+	+	-	-	+	-	+	+	-	+	+	+	-	+	+	+	+	+	+

RNAi condition

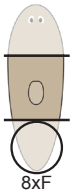

8xF
14dR

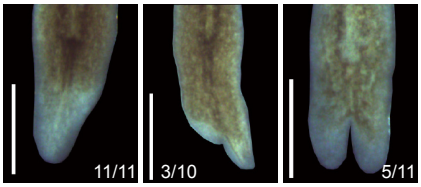

Figure S5

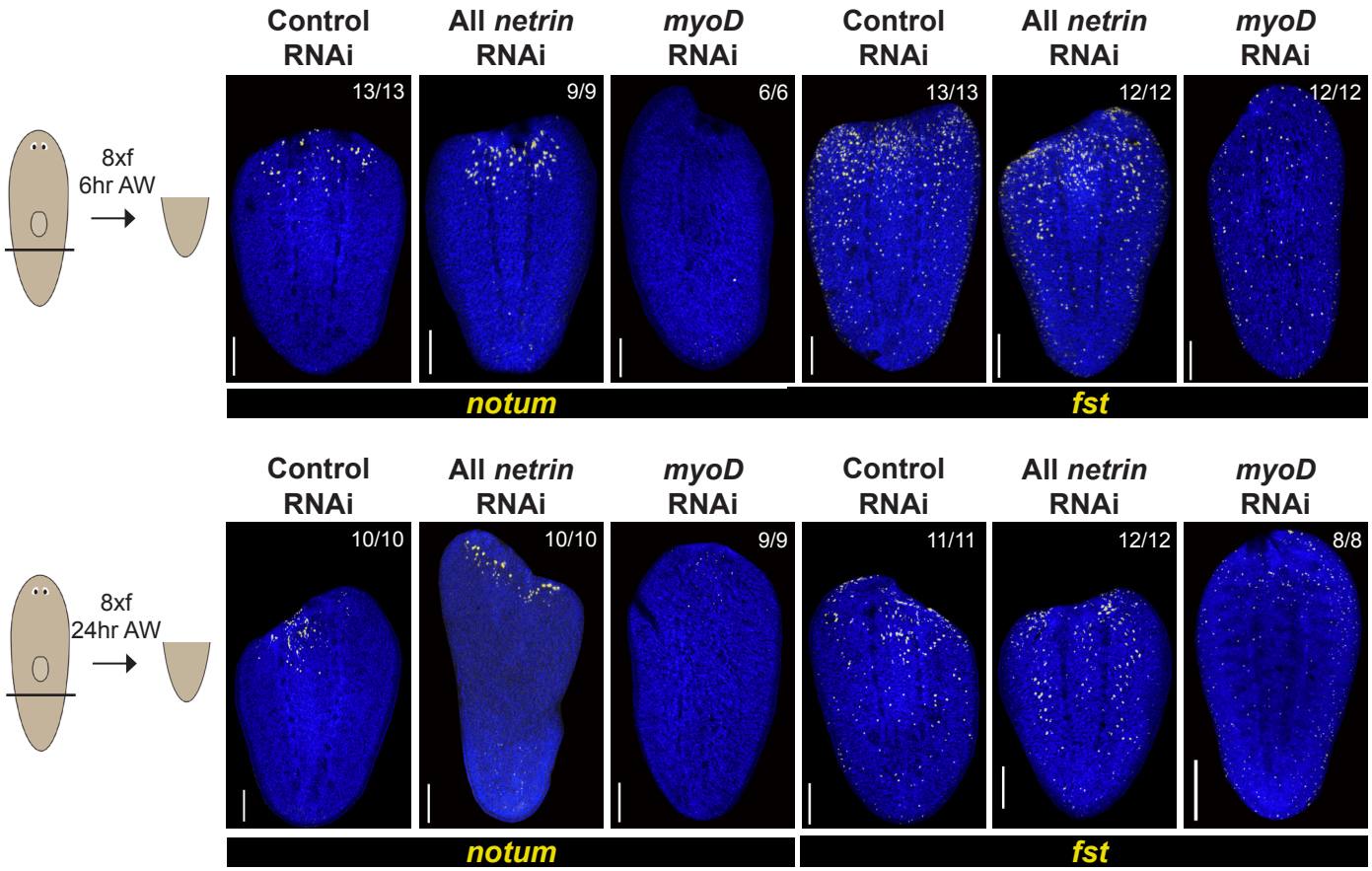
Control RNAi
All netrin RNAi
myoD RNAi
Control RNAi
All netrin RNAi
myoD RNAi
8xf
6hr AW
13/13
9/9
6/6
13/13
12/12
12/12
notum
fst
Control RNAi
All netrin RNAi
myoD RNAi
Control RNAi
All netrin RNAi
myoD RNAi
8xf
24hr AW
10/10
10/10
9/9
11/11
12/12
8/8
notum
fst